# ORIGINAL ARTICLE



Check for updates

# <sup>18</sup>O enrichment of sucrose and photosynthetic and nonphotosynthetic leaf water in a C<sub>3</sub> grass—atmospheric drivers and physiological relations

Jérôme Ogée<sup>3</sup> | Hans Schnyder<sup>1</sup>

<sup>2</sup>Forschungszentrum Jülich GmbH, Institute of Bio- and Geosciences, Agrosphere (IBG-3), Jülich, Germany

<sup>3</sup>UMR ISPA, INRAE, France

### Correspondence

Hans Schnyder and Juan C. Baca Cabrera. Email: schnyder@tum.de and j.baca.cabrera@fz-juelich.de

### **Funding information**

Deutsche Forschungsgemeinschaft

# **Abstract**

The <sup>18</sup>O enrichment ( $\Delta^{18}$ O) of leaf water affects the  $\Delta^{18}$ O of photosynthetic products such as sucrose, generating an isotopic archive of plant function and past climate. However, uncertainty remains as to whether leaf water compartmentation between photosynthetic and nonphotosynthetic tissue affects the relationship between  $\Delta^{18}$ O of bulk leaf water ( $\Delta^{18}$ O<sub>LW</sub>) and leaf sucrose ( $\Delta^{18}$ O<sub>Sucrose</sub>). We grew Lolium perenne (a C<sub>3</sub> grass) in mesocosm-scale, replicated experiments with daytime relative humidity (50% or 75%) and  $CO_2$  level (200, 400 or 800  $\mu$ mol mol<sup>-1</sup>) as factors, and determined  $\Delta^{18}O_{LW}$ ,  $\Delta^{18}O_{Sucrose}$  and morphophysiological leaf parameters, including transpiration (E<sub>leaf</sub>), stomatal conductance (g<sub>s</sub>) and mesophyll conductance to  $CO_2$  (g<sub>m</sub>). The  $\Delta^{18}O$  of photosynthetic medium water ( $\Delta^{18}O_{SSW}$ ) was estimated from  $\Delta^{18} O_{Sucrose}$  and the equilibrium fractionation between water and carbonyl groups ( $\varepsilon_{bio}$ ).  $\Delta^{18}O_{SSW}$  was well predicted by theoretical estimates of leaf water at the evaporative site ( $\Delta^{18}O_e$ ) with adjustments that correlated with gas exchange parameters (g<sub>s</sub> or total conductance to CO<sub>2</sub>). Isotopic mass balance and published work indicated that nonphotosynthetic tissue water was a large fraction (~0.53) of bulk leaf water.  $\Delta^{18}O_{LW}$  was a poor proxy for  $\Delta^{18}O_{Sucrose},$  mainly due to opposite  $\Delta^{18}$ O responses of nonphotosynthetic tissue water ( $\Delta^{18}$ O<sub>non-SSW</sub>) relative to  $\Delta^{18}O_{SSW}$ , driven by atmospheric conditions.

# KEYWORDS

 $^{18}$ O in leaf water and sucrose, atmospheric  $CO_2$  concentration, Craig-Gordon evaporative site <sup>18</sup>O enrichment, Lolium perenne (perennial ryegrass), mesophyll conductance, photosynthetic and nonphotosynthetic leaf fractions, relative humidity of air, stomatal conductance, transpiration

This is an open access article under the terms of the Creative Commons Attribution-NonCommercial License, which permits use, distribution and reproduction in any medium, provided the original work is properly cited and is not used for commercial purposes. © 2023 The Authors. Plant, Cell & Environment published by John Wiley & Sons Ltd.

<sup>&</sup>lt;sup>1</sup>Technische Universität München, TUM School of Life Sciences, Lehrstuhl für Grünlandlehre, Freising-Weihenstephan,

# 1 | INTRODUCTION

Leaf water is enriched in <sup>18</sup>O relative to source water, the water taken up by plants through their root systems (Barbour, 2007; Farquhar et al., 2007). This <sup>18</sup>O enrichment of bulk leaf water  $(\Delta^{18}O_{LW}, for definitions and specifications of symbols, see Table 1) is$ determined by environmental and biological factors (Barbour et al., 2021; Cernusak et al., 2016, 2022; Ferrio et al., 2012; Helliker & Ehleringer, 2000; 2002; Hirl et al., 2019; Holloway-Phillips et al., 2016). The <sup>18</sup>O enrichment of leaf water also affects the <sup>18</sup>O enrichment of primary photosynthetic products, such as sucrose (Cernusak et al., 2003, 2005; Lehmann et al., 2017), the most widely distributed transport sugar and primary substrate for metabolism in plants, including in grasses (Braun et al., 2014; Lalonde et al., 2003; Lattanzi et al., 2012). Although mechanistic understanding of the biological controls of  $\Delta^{18}O_{LW}$  and their relationship with  $^{18}O$ enrichment of sucrose ( $\Delta^{18}O_{Sucrose}$ ) is still imperfect, it is known that they determine an organic isotopic signal of plant function and past climate, motivating interest of a wide range of scientific disciplines from paleoecology to bioclimatology, crop physiology, ecophysiology and plant biochemistry (Barbour, 2007; Siegwolf et al., 2022). Here, our interest is to better understand the physiological controls of  $\Delta^{18}O_{LW}$  and its relationship with  $\Delta^{18}O_{Sucrose}$  in perennial ryegrass (Lolium perenne L.), a model C<sub>3</sub> grass species of high economic value (Chapman et al., 2017).

 $\Delta^{18} O_{Sucrose}$  was first assessed systematically by Cernusak et al. (2003). During steady-state leaf cuvette measurements with Ricinus communis under a range of evaporative conditions, they found a virtually constant 27‰ <sup>18</sup>O enrichment of phloem sap dry matter (which is mostly sucrose) relative to average lamina water, which is defined as bulk leaf water minus the water contained in the primary veins. This difference matched closely to expectations based on the equilibrium fractionation between water and carbonyl groups (the biochemical fractionation,  $\varepsilon_{bio}$ ) obtained in comparisons of <sup>18</sup>O in cellulose of aquatic plants and the water in which they grew (DeNiro & Epstein, 1981; Epstein et al., 1977; Yakir & DeNiro, 1990), and also in comparisons of acetone and water (Sternberg & DeNiro, 1983). Field studies with Eucalyptus globulus agreed with this finding, provided that the enrichment of average lamina water was fluxweighted over daily time scales using net CO2 assimilation rates (Cernusak et al., 2005). To our best knowledge, the relationship between  $\Delta^{18}O_{Sucrose}$  and the average lamina water of grasses has not been explored in detail. A few years ago, Lehmann et al. (2017) demonstrated that bulk leaf water of two C<sub>3</sub> grasses (L. perenne L. and Dactylis glomerata L.) is less <sup>18</sup>O enriched than the medium water where sucrose synthesis occurs ( $\Delta^{18}O_{SSW}$ ) when the latter was estimated as  $\Delta^{18}O_{Sucrose} - \varepsilon_{bio}$ , with  $\varepsilon_{bio}$  assumed to be constant at 27%. Their investigations demonstrated a systematic underestimation of  $\Delta^{18}O_{SSW}$  by  $\Delta^{18}O_{LW}$  by 3.6%-6.2% in the two species in a controlled environment study (note that Lehmann et al. used a definition of  $\Delta^{18}O_{SSW}$  which was different from the present one, since they used the <sup>18</sup>O enrichment above (bulk) leaf water rather than source water as used here). Interestingly, the offset between

 $\Delta^{18}O_{SSW}$  and  $\Delta^{18}O_{LW}$  was higher at low (50%) than at high (75%) relative humidity (RH) of the air in the growth environment.

An offset between  $\Delta^{18}O_{SSW}$  and  $\Delta^{18}O_{LW}$  is of great interest, as it can inform us about the functional heterogeneity of  $^{18}O$  enrichment of bulk leaf water (Cernusak et al., 2003; Holloway-Phillips et al., 2016; Lehmann et al., 2017) and help us to improve our understanding of the biological mechanisms controlling  $\Delta^{18}O$  of photosynthetic and sucrose synthesis medium water ( $\Delta^{18}O_{SSW}$ , Table 1) separately from nonphotosynthetic tissue water ( $\Delta^{18}O_{non-SSW}$ , Table 1) in the bulk leaf. Additionally,  $\Delta^{18}O_{SSW}$  can be compared with the modelled  $^{18}O$  enrichment at the evaporative site ( $\Delta^{18}O_e$ , see below)—as already done by Cernusak et al. (2003) in *R. communis*—to test the alternative hypothesis that  $\Delta^{18}O_{SSW}$  in grasses is closer to the  $^{18}O$  enrichment at the evaporative sites in leaves ( $\Delta^{18}O_e$ ).

 $\Delta^{18} \text{O}_e$  is modelled as (Cernusak et al., 2016, 2022; Craig & Gordon, 1965; Dongmann et al., 1974):

$$\Delta^{18}O_{e} \approx \varepsilon^{+} + \varepsilon_{k} + (\Delta^{18}O_{Vapour} - \varepsilon_{k})w_{a}/w_{i}, \tag{1}$$

with  $\varepsilon^+$  the equilibrium fractionation between liquid and vapour,  $\varepsilon_k$  the kinetic fractionation during diffusion of water vapour through the leaf boundary layer and stomata,  $\Delta^{18}O_{Vapour}$  the  $^{18}O$  enrichment of vapour above source water and  $w_a/w_i$  the ratio of the water vapour mole fractions in the air outside the leaf boundary layer and at the evaporative sites inside the leaf (Table 1).

Commonly,  $\Delta^{18}O_{LW}$  is smaller than  $\Delta^{18}O_{e}$  (Cernusak et al., 2016, 2022). This offset has been usually quantified as a proportional difference:

$$\phi_{LW} = 1 - \Delta^{18} O_{LW} / \Delta^{18} O_e.$$
 (2)

Equation 2 can be interpreted in terms of a two-pool model (Leaney et al., 1985; Song et al., 2015; Yakir et al., 1990) represented by a leaf having a certain fraction  $\phi_{LW}$  of  $^{18}\text{O}$  unenriched (source) water in the veins (or vascular and associated ground tissue) and a remaining fraction 1 –  $\phi_{LW}$  that has an  $^{18}\text{O}$  enrichment equal to that of the evaporating sites.

Conversely, Farquhar and Lloyd (1993) interpreted Equation 2 in terms of an incomplete mixing within a single-leaf water pool, with advection of less enriched water toward the evaporative sites opposing the back-diffusion (and mixing) of isotopically enriched water from those sites. By defining a Péclet number quantifying the ratio of the two opposing water isotope fluxes within the leaf mesophyll, they expressed  $\phi_{LW}$  as (Farquhar & Lloyd, 1993):

$$\phi_{LW} = 1 - (1 - e^{-\wp})/\wp,$$
(3)

where  $\wp$  is the Péclet number defined as:

$$\wp = LE/CD, \tag{4}$$

with L the effective path length of liquid water transport through the leaf, E the transpiration rate, C the molar concentration of water and D the diffusivity of heavy water ( $H_2^{18}O$ ) in water (Cernusak et al., 2016; Farquhar & Lloyd, 1993).

# TABLE 1 Definitions of symbols, and specifications.

Symbol	Definition	Specification
δ <sup>18</sup> Ο <sub>x</sub> (or δ <sup>2</sup> Η <sub>x</sub> )	The relative abundance of $^{18}$ O (or $^2$ H) in a sample X (source water, bulk leaf water or water in the LGDZ) calculated as $\delta^{18}$ O <sub>X</sub> (or $\delta^2$ H <sub>X</sub> = R <sub>X</sub> /R <sub>s</sub> – 1, with R <sub>X</sub> and R <sub>s</sub> the molar abundance ratios, $^{18}$ O $^{16}$ O (or $^2$ H $^1$ H), of the sample and of VSMOW	Tissue water in the LGDZ was collected as in Liu et al. (2017)
δ <sup>18</sup> O <sub>Source</sub> or δ <sup>2</sup> H <sub>Source</sub>	The flux-weighted average $\delta^{18}O/\delta^2H$ of the water taken up by the root system of a plant, often termed $\delta^{18}O/\delta^2H$ of xylem water	$\delta^{18}$ O of nutrient solution (-9.7 ± 0.2% SD); $\delta^2$ H of nutrient solution (-70.1 ± 1.2% SD)
$\delta^{18}$ Ovapour or $\delta^2$ Hvapour	The $\delta^{18} O/or  \delta^2 H$ of vapour as measured above the canopy	$\delta^{18}O_{Vapour}/\delta^2H_{Vapour}$ constant across experimental runs and treatments, but more enriched during the dark period ( $\delta^{18}O = -14.2\% \pm 0.5\%$ SD; $\delta^2H = -104.6\% \pm 3.8\%$ SD) than during the light period ( $\delta^{18}O = -15.2\% \pm 0.6\%$ SD; $\delta^2H = -109.6\% \pm 4.4\%$ SD)
$\Delta^{18} O_{\chi}$	The $^{18}O$ enrichment above source water of a sample X (leaf water, LGDZ water, sucrose or vapour) calculated as $\Delta^{18}O_{X}=(\delta^{18}O_{X}-\delta^{18}O_{Source})/(1+\delta^{18}O_{Source})$	
$\Delta^{18} O_{LW}$	The $\Delta^{18}\!\!$ O of bulk leaf blade water	
$\Delta^{18} O_{\rm SSW}$	The $\Delta^{18}\!$	Estimated as $\Delta^{18} O_{Sucrose}$ – $\epsilon_{bio}$
$\Delta^{18} O_{\text{non-SSW}}$	The $\Delta^{18} \! O$ of water in the total nonphotosynthetic fraction of the leaf blade	Calculated by isotopic mass balance (Equation 15, $\Delta^{18} O_{\text{non-SSW}} = (\Delta^{18} O_{\text{LW}} - f_{\text{SSW}} \Delta^{18} O_{\text{SSW}}) / f_{\text{non-SSW}})$ using replicate-specific data of $\Delta^{18} O_{\text{LW}}$ , $\Delta^{18} O_{\text{SSW}}$ and estimates of the nonphotosynthetic bulk leaf water fraction ( $f_{\text{non-SSW}}$ ) of Lolium perenne leaf blades
€bio	The average biochemical fractionation between carbonyl oxygen and water	26.7%, according to the temperature dependence of $\epsilon_{\rm bio}$ for cellulose synthesis in aquatic plants as reported by Sternberg and Ellsworth (2011); constant for all treatments and closely similar to the constant $\epsilon_{\rm bio}=27\%$ used in most studies (Barbour, 2007)
$\Delta^{18}O_{\mathrm{e}}$	Theoretical estimate of the transpiration-weighted $\Delta^{18}\text{O}$ at the evaporative site of whole-leaf blades (Farquhar & Gan, 2003)	Estimated using Equation 1: $\Delta^{18}O_e \approx \epsilon^+ + \epsilon_k + (\Delta^{18}O_{vapour} - \epsilon_k) \; w_a/w_h,$ assuming: cuticular transpiration did not occur, stomatal conductance was nonpatchy and there were no gradients in leaf temperature, relative humidity and stomatal conductance inside the canopies
<sup>‡</sup> ω	The equilibrium fractionation between liquid and vapour phase	Estimated according to Majoube (1971): $ \epsilon^* = \left[ \exp \left( \frac{1137}{273 + 77} - \frac{415.6}{273 + 77} - 2066.7 \right) - 1 \right] \times 1000, $ with $T$ the measured leaf temperature
చ	The kinetic fractionation during diffusion of water vapour through the leaf boundary layer and stomata	Calculated as in Farquhar et al. (1989) $\epsilon_k = \frac{28_8 + 197_b}{r_b + r_b},$ with $r_s$ and $r_b$ the stomatal and boundary layer resistances, respectively (inverses of stomatal and boundary layer conductances)
wa∕w <sub>i</sub>	The ratio of the water vapour mole fractions in the air outside the leaf boundary layer and at the evaporative sites inside the leaf	

(Continued)		
IABLE 1		

Symbol	Definition	Specification
×	The proportional difference between $\Delta^{18}O_X$ (the $\Delta^{18}O$ of a sample X) and $\Delta^{18}O_e$ (i.e., $\phi_X$ = $1$ – $\Delta^{18}O_X/\Delta^{18}O_e$ ), with X representing either bulk leaf blade, SSW or non-SSW water	
7	The effective path length of liquid water transport through the leaf	Calculated by solving Equations 4 and 7: $L = \&OD/E, \\ \wp = -\ln \frac{ {\it \Delta}^{18} O_L w - (1 - f_{non-SSW}) {\it \Delta}^{18} O_e}{f_{non-SSW} {\it \Delta}^{18} O_e}, \text{ with } \\ E the transpiration rate, C the molar concentration of water and D the diffusivity of heavy water (H2^{18}O) in water$
$f_{x}$ ; $(1 - f_{x})$	The fraction of vein water in bulk leaf water; $(1$ – $f_x)$ the remaining leaf water	
fsswi fnon-ssw	The photosynthetic (and sucrose synthesis) water (SSW) and nonphotosynthetic water (non-SSW) fractions of bulk leaf blade water ( $f_{non-SSW}=1-f_{SSW}$ )	f <sub>non-SSW</sub> = 0.53 estimated as the fraction of nonmesophyll water in bulk leaf blade water of <i>L. perenne</i> according to published leaf anatomy data (Charles-Edwards et al., 1974; Dengler et al., 1994) and used in Equation 6 under the standard assumption of a well-mixed mesophyll. In a sensitivity analysis (Figure 4, see also Figure 7) we also used f <sub>non-SSW</sub> = 0.70 and 0.88 to assess putative effects of a nonfully-mixed mesophyll
8s H <sub>2</sub> O	Stomatal conductance to $H_2O$	From leaf level measurements under the same environmental conditions as in the growth chambers for each treatment
8s co <sub>2</sub>	Stomatal conductance to CO <sub>2</sub>	As specified for $g_{s \; H_2O}$ , above
g <sub>m</sub>	Mesophyll conductance to ${ m CO}_2$	Estimated using the $^{13}\mathrm{C}$ discrimination method (Evans et al., 1986) during parallel $g_\mathrm{s}$ and $E_\mathrm{leaf}$ measurements
gtotal	Total conductance for CO <sub>2</sub> , estimated as the sum of $g_{\rm sco_2}$ and $g_{\rm m}$	Calculated as $1/(1/g_{sCO_2}+1/g_m)$
Eleaf	Leaf transpiration rate	From leaf level measurements under the same environmental conditions as in the growth chambers for each treatment
- 100		

Abbreviations: LGDZ, leaf growth-and-differentiation zone; SD, standard deviation; SSW, sucrose synthesis water; VSMOW, Vienna standard mean ocean water.

.3653040, 2023, 9, Downloaded from https:

, Wiley Online Library

on [25/08/2023]. See the Terms

Recently, Barbour et al. (2021) investigated the relationship between transpiration and  $\phi_{LW}$  in 21 species from different functional groups, testing the prediction that detection of the Péclet effect represented by Equation 3 is dependent on leaf hydraulic design. This analysis included one C<sub>3</sub> grass species, wheat (Triticum aestivum L.), which is characterized by relatively weak hydraulic connections between veins, mesophyll and epidermal cells (Barbour et al., 2021). In this analysis of wheat, transpiration and  $\varphi_{LW}$  were not systematically related, similar to other species with the same leaf hydraulic design. For these species, Barbour et al. (2021) suggested that more complex models may be required that represent hydraulically disconnected pools. Holloway-Phillips et al. (2016) described a two-pool variant of such a bulk leaf water  $\Delta^{18}$ O model (defined by their Equation 9), that considers very slow movement of water through the symplast of the mesophyll fraction of the leaf (leading to equilibration of mesophyll water and hence sucrose with evaporative site water) and a vein fraction that displays a Péclet effect:

$$\Delta^{18}O_{LW} = (1 - f_x)\Delta^{18}O_e + f_x\Delta^{18}O_e e^{-\wp_r},$$
 (5)

with  $f_x$  the leaf water fraction in the veins,  $(1 - f_x)$  the remaining leaf water fraction (lamina) which includes the mesophyll, and  $\wp_r$  a radial Péclet number.

The data of Lehmann et al. (2017) are also consistent with a two-pool model in that they imply differential RH responses of  $\Delta^{18}$ O in two functionally distinct tissue water fractions: the photosynthetic medium water fraction, where sucrose synthesis takes place ( $f_{SSW} = 1 - f_{non-SSW}$ ), and the remaining 'nonphotosynthetic' leaf water fraction that includes the veins ( $f_{non-SSW}$ ):

$$\Delta^{18}O_{LW} = (1 - f_{non-SSW})\Delta^{18}O_{SSW} + f_{non-SSW}\Delta^{18}O_{non-SSW}.$$
 (6)

In the hypothetical case that  $\Delta^{18}O_{SSW} = \Delta^{18}O_e$  (i.e.,  $\phi_{SSW} = 1 - \Delta^{18}O_{SSW}/\Delta^{18}O_e = 0$ ) this model may be expressed analogous to Equation 5 as:

$$\Delta^{18}O_{LW} = (1 - f_{non-SSW})\Delta^{18}O_{e} + f_{non-SSW}\Delta^{18}O_{e}e^{-\wp_{r}}.$$
 (7)

However, anatomical literature shows that  $f_{\text{non-SSW}}$  is much greater than  $f_x$  (and, hence,  $f_{\text{SSW}}$  is much smaller than  $1-f_x$ ), illustrating the fact that using Equation 7 allows a better accounting of the nonphotosynthetic fraction of bulk leaf water in the two-pool model. According to studies of Charles-Edwards et al. (1974) with L. perenne the vascular tissue ( $\approx f_x$ ), including parenchyma extensions and bundle sheath, accounted for ~10% of the leaf cross-sectional area and ~12% of bulk leaf water, considering that intercellular air space accounts for ~30% of the mesophyll volume (Dengler et al., 1994). On the same basis, the epidermis accounted for ~41% and the mesophyll for ~47% of bulk leaf water content (LWC). On this basis, the sum of vascular tissue and epidermis (which together represent  $f_{\text{non-SSW}}$ ) accounts for a total of ~53% of the bulk leaf water in L. perenne, mainly due to the dominant contribution of the epidermis. Considering that (1) hydraulic connections between

mesophyll and surrounding tissue may be weak in grasses (or in other species with the same hydraulic design; Barbour et al., 2021; Zwieniecki et al., 2007), and (2) expectations from Equation 5, that is, that the mesophyll is well-mixed (cf eq. 9 in Holloway-Phillips et al., 2016), we hypothesize that Equation 7 is a useful abstraction of  $\Delta^{18}O_{LW}$  based on  $\Delta^{18}O$  in its component photosynthetic ( $\Delta^{18}O_{SSW}$ ) and nonphotosynthetic tissue water fractions ( $\Delta^{18}O_{non-SSW}$ ).

In this context, this work addresses five questions. First, it compares  $\Delta^{18}O_{SSW}$  (estimated as  $\Delta^{18}O_{Sucrose}$  –  $\epsilon_{bio}$  ignoring secondary isotope terms) with  $\Delta^{18}O_{LW}$  in the  $C_3$  grass L. perenne, one of the model species used by Lehmann et al. (2017), to corroborate their finding of an RH-dependent mismatch between  $\Delta^{18}O_{SSW}$  and  $\Delta^{18}O_{LW}$ . Second, it analyzes the relationship between  $\Delta^{18}O_{SSW}$  and  $\Delta^{18} O_e,$  to test the hypothesis that  $\Delta^{18} O_{SSW}$  is more closely associated with  $\Delta^{18} O_e$  than with  $\Delta^{18} O_{LW}$  in L. perenne, similar to the approach used by Cernusak et al. (2003) with a dicot species, R. communis. Third, we solve Equation 6 for  $\Delta^{18}O_{non\text{-SSW}}$  , using  $\Delta^{18}O_{LW}$  $\Delta^{18}O_{SSW}$  and the estimate of the fraction of nonphotosynthetic tissue water ( $f_{non-SSW}$ ) of 0.53 (see above and Charles-Edwards et al., 1974; Dengler et al., 1994). In that, we also test the sensitivity of  $\Delta^{18}O_{\text{non-SSW}}$  to the assumption (in Equation 7) that the mesophyll is well-mixed, by including some mesophyll (e.g., mesophyll vacuole volume) in the non-SSW fraction. Fourth, we evaluate the proportional difference between estimates of  $\Delta^{18}O_{non\text{-SSW}}$  and  $\Delta^{18}O_{e}$   $(\phi_{non\text{-}}$  $_{SSW} = 1 - \Delta^{18}O_{non-SSW}/\Delta^{18}O_e$ ) and its sensitivity to the well-mixed mesophyll assumption. Finally, we explore the relationship between  $\phi_{SSW}$  or  $\phi_{non\text{-}SSW}$  and physiological parameters (including transpiration and stomatal and mesophyll conductances) that have been implied previously as putative controls of  $\phi_{\text{LW}}.$  In that, we also explore the idea that nonphotosynthetic leaf water displays a Péclet effect (based on Equation 7) and discuss possible implications for the sites of evaporation within leaves (Barbour et al., 2017; Barbour et al., 2021; Rockwell et al., 2014) in contrasting atmospheric CO2 concentration and daytime RH. This work made use of a fully replicated (n = 3-5) mesocosm-scale experiment described previously by Baca Cabrera et al. (2020) with L. perenne plants grown in swardlike conditions in a 2 × 3 factorial experiment with atmospheric CO<sub>2</sub> concentration (200, 400 or 800 µmol mol<sup>-1</sup>) and daytime RH of 50% or 75%.

# 2 | MATERIALS AND METHODS

# 2.1 | Plant material and growth conditions

Perennial ryegrass (*L. perenne*, cv. 'Acento') plants were grown in four plant growth chambers (PGR15; Conviron) in a 16: 8 h day: night cycle (temperature 20/16°C), under a  $3 \times 2$  factorial design: three atmospheric  $CO_2$  concentration levels ('half-ambient' = 200, 'ambient' = 400 or 'double-ambient' = 800  $\mu$ mol mol<sup>-1</sup>) and two daytime RH levels (low RH = 50%, high RH = 75%; nighttime RH was 75% for all treatments), as previously described in Baca Cabrera et al. (2020). In brief, *L. perenne* plants were grown individually in plastic tubes



(350 mm height, 50 mm diameter) filled with washed quartz sand (0.3–0.8 mm grain size) and arranged in plastic containers (770 × 560 × 300 mm) at a density of 383 plants m $^{-2}$ . Plants were supplied four times a day with a Hoagland-type nutrient solution with reduced nitrate-N content. Light was supplied by cool-white fluorescent tubes and warm-white light-emitting diode (LED) bulbs with a constant photosynthetic photon flux density (PPFD) of 800  $\mu$ mol m $^{-2}$  s $^{-1}$  at plant height during the 16 h-long light period. A total of five sequential experimental runs were performed, resulting in five chamber scale replicates for the so-called 'reference treatment' (400  $\mu$ mol mol $^{-1}$  CO $_2/50\%$  RH) and three replicate mesocosm-scale runs for the other treatments.

CO2 and RH treatments were installed on the 13th day after seed imbibition. For this, the air supplied to the chambers was mixed from dry CO<sub>2</sub>-free air and <sup>18</sup>O-enriched or <sup>18</sup>O-depleted tank CO<sub>2</sub>. using mass flow controllers. <sup>18</sup>O-enriched CO<sub>2</sub> was obtained from CARBO Kohlensäurewerke and had a δ<sup>18</sup>O<sub>CO2</sub> which ranged between 14.1% and 20.2% between individual cylinders:  $^{18}\text{O-depleted}$  CO $_2$  was purchased from Linde AG and had a  $\delta^{18} O_{CO2}$  which ranged between -9.0% and -2.0% between individual cylinders. In each experimental run, treatments were run in duplicate, with one chamber receiving the <sup>18</sup>O-depleted and the other chamber the <sup>18</sup>O-enriched CO<sub>2</sub>. RH and temperature were controlled by the chamber control system (CMP6050; Conviron). CO<sub>2</sub> concentration and RH were measured every 30 min by an infrared gas analyzer (IRGA; Li-840; Li-Cor) and never deviated more than ±5 umol mol<sup>-1</sup> and ±2.0% relative to the set nominal value. respectively. The  $\delta^{18}$ O of CO<sub>2</sub> at the inlet and outlet of each growth chamber was measured as in Liu et al. (2016) with a continuous-flow isotope ratio mass spectrometer (IRMS) (Delta Plus, Finnigan MAT).

# 2.2 | Sampling design and extraction of tissue water and sucrose

Plants from each chamber-scale replicate were sampled when plant canopies were closed (leaf area index >5, at 7–9 weeks after the beginning of the experiment). At that time, the morphometric traits of leaves were similar among treatments (Baca Cabrera et al., 2020). Sampling took place at c. 2 h before the end of the light and dark periods. In each replicate sampling, 12 plants were randomly selected, dissected and the sampled plant material of 6 plants pooled in 1 subsample (providing 2 subsamples per chamber and per sampling occasion). Additionally, we sampled other plants as described in Baca Cabrera et al. (2020), to estimate LWC (in mol m<sup>-2</sup> leaf area) of young fully expanded leaf blades. LWC was obtained gravimetrically and normalized by the leaf area. The IMAGE J software (Schneider et al., 2012) was used for digital analysis.

For tissue water extraction, the two youngest fully expanded leaf blades and the leaf growth-and-differentiation zone (LGDZ, see Figure 1 in Baca Cabrera et al., 2020) of three mature tillers per plant were excised, sealed in  $12\,\text{mL}$  Exetainer vials (Labco), capped, wrapped with Parafilm and stored at  $-18^{\circ}\text{C}$  until water extraction.

Tissue water was extracted for 2 h using cryogenic vacuum distillation as in Liu et al. (2016).

For sucrose extraction, the youngest fully expanded leaf blades of another two mature tillers from the same plants were excised, placed into paper bags, frozen in liquid nitrogen, stored at -18°C until freeze-drying, milled and stored again at -18°C until sucrose extraction. Water-soluble carbohydrates were extracted from 50 mg aliquots of dry material and sucrose separated from other compounds using a preparative high-performance liquid chromatography (HPLC) technique according to Gebbing and Schnyder (2001).

Using separate samples for tissue water and sucrose extraction could theoretically lead to greater scatter in the relationship between  $\delta^{18} O$  of leaf water ( $\delta^{18} O_{LW}$ ) and sucrose ( $\delta^{18} O_{Sucrose}$ ), an eventuality that we minimized by extensive subsampling.

# 2.3 | Gas exchange measurements

Leaf gas exchange measurements were performed during a 2-week interval between weeks 7 and 9 as described in Baca Cabrera et al. (2020). In brief, net assimilation (A, µmol CO<sub>2</sub> m<sup>-2</sup> s<sup>-1</sup>), leaf transpiration (E<sub>leaf</sub>, mmol H<sub>2</sub>O m<sup>-2</sup> s<sup>-1</sup>) and stomatal conductance to water vapour or  $CO_2$  ( $g_{s H_2O}$ , mol  $H_2O m^{-2} s^{-1}$  or  $g_{s CO_2}$ , mol CO<sub>2</sub> m<sup>-2</sup> s<sup>-1</sup>) were measured on 6-12 plants per treatment with a LI-6400xt (Li-Cor) portable CO<sub>2</sub>/H<sub>2</sub>O gas exchange system with a clamp-on leaf cuvette (2 × 3 cm), installed in a separate plant growth chamber (E15, Conviron). For measurements, individual plants were removed from their growth chamber, and the midsection of the youngest fully developed leaf blades of four tillers was enclosed in the leaf cuvette. A,  $g_s$  and  $E_{leaf}$  were measured at a leaf temperature of 21°C (air temperature in the leaf cuvette ranged between c. 20.0-21.0°C) and a PPFD of 800  $\mu$ mol m<sup>-2</sup> s<sup>-1</sup> and with CO<sub>2</sub> concentration and RH in the leaf cuvette (sample chamber) set equal to the conditions in the original growth environment.

Air for the leaf cuvette was supplied by mixing  $CO_2$ -free, dry air (with 21%  $O_2$ ) and tank  $CO_2$  (from Carbo Kohlensäurewerke or Linde AG, see Section 2.1) using mass flow controllers. Measurements were logged under steady-state conditions for stomatal conductance and water vapour concentration.

# 2.4 | Mesophyll conductance to CO<sub>2</sub>

Mesophyll conductance to CO<sub>2</sub> ( $g_m$ ) was calculated using the on-line carbon discrimination method (Evans et al., 1986; Flexas et al., 2013).  $^{13}\text{CO}_2/^{12}\text{CO}_2$  leaf gas exchange was measured by coupling the leaf cuvette system to an online gas IRMS (Delta plus, Finnigan MAT), using the protocols described in Gong et al. (2015). Online  $^{13}\text{C}$  discrimination during photosynthesis ( $\Delta^{13}\text{C}$ ) was calculated according to Evans et al. (1986).  $g_m$  was estimated based on the difference between the observed  $\Delta^{13}\text{C}$  ( $\Delta_{\text{obs}}$ ) and the theoretical  $\Delta^{13}\text{C}$  model of Farquhar et al. (1982), assuming an infinite  $g_m$  ( $\Delta_{\text{inf}}$ ).  $\Delta_{\text{inf}}$  was calculated by including the ternary effect (Farquhar & Cernusak, 2012) as:

$$\Delta_{inf} = \frac{1}{1 - t} \left( a_b \frac{c_a - c_s}{c_a} + a_s \frac{c_s - c_i}{c_a} \right) + \frac{1 + t}{1 - t} \left( b \frac{c_i}{c_a} - \frac{\alpha_b}{\alpha_e} e \frac{R_d}{A + R_d} \frac{c_i - \Gamma^*}{c_a} - \frac{\alpha_b}{\alpha_f} f \frac{\Gamma^*}{c_a} \right),$$
(8)

where  $c_a$ ,  $c_s$  and  $c_i$  are the CO<sub>2</sub> mole fractions in the atmosphere, at leaf surface and in the substomatal cavity, respectively; A is net photosynthesis,  $R_d$  represents day respiration rate,  $\Gamma^*$  is the CO<sub>2</sub> compensation point in the absence of mitochondrial respiration (calculated as in Bernacchi et al., 2001);  $a_b$  and  $a_s$  are the carbon isotope discriminations caused by diffusion through the boundary layer (2.9‰) and stomata (4.4‰), respectively; b (28.9‰, McNevin et al., 2006), e (0‰–5‰, Ubierna et al., 2018) and f (11.6‰, Lanigan et al., 2008) represent the discrimination due to carboxylation, daytime mitochondrial respiration and photorespiration, respectively;  $a_b = 1 + b$ ,  $a_e = 1 + e$  and  $a_f = 1 + f$ ; and t is the ternary correction factor calculated as:

$$t = \frac{(1 + a_{ac})E}{2g_{ac}},$$
 (9)

$$a_{ac} = \frac{a_b(c_a - c_s) + a_s(c_s - c_i)}{c_a - c_i},$$
 (10)

where E is the transpiration rate and  $g_{\rm ac}$  is the combined boundary layer and stomatal conductance to  $CO_2$ . Under the assumption that the impact of day respiration is negligible (e = 0) under the measurement conditions (Ma et al., 2021; Ubierna et al., 2018) Equation 7 can be simplified to:

$$\Delta_{\inf} = \frac{1}{1 - t} \left( a_b \frac{c_a - c_s}{c_a} + a_s \frac{c_s - c_i}{c_a} \right) + \frac{1 + t}{1 - t} \left( b \frac{c_i}{c_a} - \frac{\alpha_b}{\alpha_f} f \frac{\Gamma^*}{c_a} \right), \tag{11}$$

and  $g_m$  was calculated as:

$$g_{\rm m} = 1/\left[\frac{1-t}{1-t}(\Delta_{\rm inf} - \Delta_{\rm obs})\frac{c_{\rm a}}{A(b-a_{\rm m})}\right],$$
 (12)

with  $a_{\rm m}$  (1.8%, O'Leary, 1984) the discrimination during CO<sub>2</sub> dissolution and diffusion in the mesophyll.

# 2.5 | Isotope analysis

Oxygen (or hydrogen) isotope composition was expressed in per mil (‰) as:

$$\delta^{18}O(\text{or}\delta^2H) = \left(\frac{R_{\text{sample}}}{R_{\text{standard}}} - 1\right) \times 1000, \tag{13}$$

with  $R_{\text{sample}}$  the  $^{18}\text{O}/^{16}\text{O}$  (or  $^2\text{H}/^1\text{H}$ ) ratio of the sample and  $R_{\text{standard}}$  that in the international standard (Vienna Standard Mean Ocean Water, V-SMOW).  $\delta^{18}\text{O}$  and  $\delta^2\text{H}$  were measured in the following compartments: tissue water of leaf blades ( $\delta^{18}\text{O}_{\text{LW}}$  and  $\delta^2\text{H}_{\text{LW}}$ ) and of the LGDZ ( $\delta^{18}\text{O}_{\text{LGDZ}}$  and  $\delta^2\text{H}_{\text{LGDZ}}$ ) and nutrient solution ( $\delta^{18}\text{O}_{\text{Source}}$  and  $\delta^2\text{H}_{\text{Source}}$ ). Sucrose samples extracted from leaf blades were only measured for  $^{18}\text{O}$  ( $\delta^{18}\text{O}_{\text{Sucrose}}$ , see below). The nutrient solution was

sampled once or twice weekly.  $\delta^{18}O_{Source}$  and  $\delta^2H_{Source}$  were near constant throughout the experiment (-9.7 ± 0.2% and -70.1 ± 1.2% SD, respectively).  $\delta^{18}O_{Source}$  was used to calculate <sup>18</sup>O enrichment above source water ( $\Delta^{18}O_X$  per mil) of the different samples (X) as:

$$\Delta^{18}O_X = \frac{\delta^{18}O_X - \delta^{18}O_{\text{Source}}}{1 + \delta^{18}O_{\text{Source}}/1000}.$$
 (14)

Water samples were analyzed by cavity ring-down spectroscopy as described in Liu et al. (2016). A total of 1  $\mu L$  of a water sample was injected into an A0211 high-precision vapourizer coupled to an L2110-i-CRDS (both Picarro Inc.). Each sample was measured 5–12 times depending on memory effects. After every 15–25 samples, heavy and light laboratory water standards, spanning the range of  $\delta^{18}O$  values in the data set and previously calibrated against V-SMOW, V-GISP and V-SLAP, were measured for SMOW-scaling and possible drift correction. Analytical uncertainty (standard deviation, SD) was <0.2% and <1.0% for  $\delta^{18}O$  and  $\delta^2H$ , respectively.

Sucrose samples were measured by isotope ratio mass spectrometry (IRMS) as in Baca Cabrera et al. (2021). Each sample was measured against a laboratory working standard carbon monoxide gas, previously calibrated against a secondary isotope standard (IAEA-601, accuracy of calibration ±0.25% SD). Solid internal laboratory standards (cotton powder) were run each time after the measurement of four samples for possible drift correction and for SMOW-scaling. The precision (SD) for the laboratory standard was <0.3%.

We also checked for possible fractionation effects during HPLC sucrose separation, by comparing untreated fine ground sucrose directly weighed into silver cups with the same sucrose obtained after passage through the HPLC column. For the latter, we prepared a standard-mix (containing fructan, sucrose, glucose and fructose in typical tissue concentrations) and collected the sucrose fraction eluting from the HPLC column. No difference was detected for  $\delta^{18}O_{\text{Sucrose}}$  of the untreated sucrose (30.8  $\pm$  0.7% SD) compared with the sucrose from the standard-mix passed through the HPLC (31.0  $\pm$  0.3% SD).

Additionally,  $\delta^{18}O$  and  $\delta^{2}H$  of water vapour in the growth chambers  $(\delta^{18}O_{Vapour}/\delta^{2}H_{Vapour})$  was measured by cavity ring-down spectroscopy as described in Liu et al. (2016). Here, we measured  $\delta^{18}O_{Vapour}/\delta^{2}H_{Vapour}$  continuously for 2 weeks when canopies were closed, both during the light and the dark periods.  $\delta^{18}O_{Vapour}$  was constant across experimental runs and treatments but was c. 1% more enriched during the dark period (–14.2%  $\pm$  0.5% SD) than during the light period (–15.2%  $\pm$  0.6% SD). A similar behaviour was observed for  $\delta^{2}H_{Vapour}$  (–104.6%  $\pm$  3.8% SD during the dark period and –109.6%  $\pm$  4.4% SD during the light period).

# 2.6 | Evaporative site <sup>18</sup>O enrichment

The  $^{18}\text{O}$  enrichment of evaporative sites water above source water  $(\Delta^{18}\text{O}_e)$  during the light period was calculated using the Craig–Gordon model (Craig & Gordon, 1965; Dongmann et al., 1974) as presented in Cernusak et al. (2016) and given in Equation 1.  $w_a/w_i$  was calculated based on daytime air temperature (20°C) and RH (50% or 75%) inside the chambers, and canopy surface temperature, which was estimated using



measurements of six type T thermocouples (in-house, custom-made) attached to mature leaf blades across each canopy.  $\epsilon^+$  and  $\epsilon_k$  were calculated as in Cernusak et al. (2016) (see Table 1), with stomatal conductance and boundary layer conductance  $(g_b)$  data obtained from leaf gas exchange measurements and rates of water loss from leaf replicas (Grace & Wilson, 1976)  $(g_b \approx 0.2 \, \text{mol m}^{-2} \, \text{s}^{-1}$  for all treatments), respectively. Calculation of  $\Delta^{18} O_e - \text{as}$  given here—makes the (customary) simplifying assumptions that cuticular transpiration did not occur, stomatal conductance was nonpatchy and there were no gradients in leaf temperature, RH and stomatal conductance between the base and the top of the canopies.

# 2.7 | The fractions of leaf water in nonphotosynthetic leaf tissue and its <sup>18</sup>O enrichment

According to isotopic mass balance,  $\Delta^{18}O_{LW}$  is a mass-weighted average of the  $\Delta^{18}$ O of its photosynthetic ( $\Delta^{18}$ O<sub>SSW</sub>) and nonphotosynthetic ( $\Delta^{18}O_{non\text{-SSW}}$ ) components, with  $f_{ssw}$  and  $f_{non\text{-SSW}}$  the mass fractions of photosynthetic and nonphotosynthetic leaf water  $(f_{\text{non-SSW}} = 1 - f_{\text{SSW}})$  (Equation 6).  $\Delta^{18}O_{LW}$  was obtained experimentally as explained above, and  $\Delta^{18}O_{SSW}$  was estimated as  $\Delta^{18} O_{Sucrose}$  –  $\epsilon_{bio},$  with  $\epsilon_{bio}$  the  $^{18} O$  fractionation between carbonyl groups and water in which they are formed (Barbour, 2007).  $\varepsilon_{bio}$ (=26.7%) was estimated from the temperature-dependence of  $\varepsilon_{bio}$ associated with cellulose synthesis in aquatic plants (Sternberg & Ellsworth, 2011; see also Hirl et al., 2021) and the nominal daytime air temperature in the growth chambers (including treatment-related offsets of canopy temperature in the calculation would not change the temperature-dependent  $\varepsilon_{bio}$  by more than  $\pm$  0.15%). This estimate of  $\varepsilon_{bio}$  is also close to the (temperature-independent, constant) 27% which has been used most commonly in this type of analysis (Barbour, 2007; Lehmann et al., 2017).

 $\Delta^{18}O_{non-SSW}$  was estimated by solving Equation 6 as:

$$\Delta^{18}O_{\text{non-SSW}} = (\Delta^{18}O_{\text{LW}} - f_{\text{SSW}}\Delta^{18}O_{\text{SSW}})/f_{\text{non-SSW}}, \tag{15}$$

with  $f_{\text{non-SSW}}$  set to 0.53, the anatomically based estimate of the proportion of nonmesophyll tissue in bulk leaf water, obtained from leaf cross-sections of different cultivars of L. perenne grown at different temperatures and light intensities (Charles-Edwards et al., 1974), corrected for an average 30% contribution of intercellular air spaces in  $C_3$  grasses to mesophyll volume (Dengler et al., 1994, see Section 1). This estimation uses the assumption that the fractional area of water-filled tissue equals water volumetric fraction, which demands that cross-sections were representative for longitudinal variation of mesophyll and nonmesophyll tissue. Further, when predicting  $\Delta^{18}O_{\text{non-SSW}}$  with Equation 7, the use of  $f_{\text{non-SSW}} = 0.53$  assumes a perfectly well-mixed mesophyll water pool.

To allow for and explore the uncertainty of this well-mixed mesophyll assumption, we also used higher values of  $f_{\text{non-SSW}}$ , which effectively treated part of the mesophyll (e.g., some or all the mesophyll vacuole volume) as a component of the nonmesophyll fraction, that is, reflecting a  $\Delta^{18}\text{O}$  equal to that of the nonmesophyll water ( $\Delta^{18}\text{O}_{\text{non-SSW}}$ ). The most

extreme scenario set  $f_{\text{non-SSW}} = 0.88$ , which would include the entire mesophyll vacuole volume in the nonmesophyll fraction. In this scenario, the photosynthetic leaf water fraction ( $f_{\text{SSW}}$ ) equaled 0.12 and was represented solely by the combined water volume fraction of the mesophyll cytosol and chloroplasts. The latter was calculated from the volume fraction of cytosol *plus* chloroplasts (26%) in mesophyll cells of barley leaves (Winter et al., 1993) as 0.26 × (1 – 0.53). As an intermediate scenario we used  $f_{\text{non-SSW}} = 0.70$ . These higher estimates of  $f_{\text{non-SSW}}$  were then used to analyze the sensitivity of  $\Delta^{18}O_{\text{non-SSW}}$  (Equation 15),  $\phi_{\text{non-SSW}}$  (=1  $\Delta^{18}O_{\text{non-SSW}}/\Delta^{18}O_{\text{e}}$ ) and effective path length (L; calculated by the Péclet effect model defined by Equation 7) to variation of  $f_{\text{non-SSW}}$ .

# 2.8 | Data selection and statistics

In the first step, linear mixed models were fitted to test the effect of the diel period (day vs. night) on  $\Delta^{18}O_{LW}$  (n = 160) and  $\Delta^{18}O_{SSW}$  (n = 70). All available subsamples (pseudo-replicates) were included in the analysis, with the growth chamber and experimental run defined as the random factors. A small but significant diel trend between the end of the light period and the end of the dark period was detected for  $\Delta^{18}O_{LW}$ , but not for  $\Delta^{18}O_{SSW}$  (Supporting Information: Table S1). Therefore, we decided to: (1) pool day and night  $\Delta^{18}O_{SSW}$  data together; and (2) only use  $\Delta^{18}O_{LW}$  data obtained near the end of the light period for further calculations, under the assumptions that these values better reflect <sup>18</sup>O enrichment processes during photosynthesis. Additionally, we calculated  $\phi_{LW}$  and  $\phi_{non-SSW}$  (which are derived from  $\Delta^{18}O_{LW}$ ) using data obtained either near the end of the light or the dark period but observed only very small differences and no variation in the CO2 and RH statistical effects on these variables (Supporting Information: Figure S1), indicating that our data selection was reasonable for further analyses.

In a second step, canopy scale replicates were obtained by pooling all individual subsamples from each canopy (n = 3–5) and two-way analysis of variance (ANOVA) tests used to assess the effects of CO<sub>2</sub>, RH and their interaction on  $\Delta^{18}O_{LW}$ ,  $\Delta^{18}O_{SSW}$ ,  $\Delta^{18}O_{e}$  and all derived parameters. The same statistical analysis was used for the gas exchange parameters but based on individual leaf replicates (n = 6–12). Additionally, ordinary least-squares linear regressions were performed to test the relationship between the different parameters (using treatment averages). All statistical analyses were performed in R v.4.0.2 (R Core Team, 2022). The R packages nlme (Pinheiro et al., 2019) and ggplot2 (Wickham, 2016) were used for fitting linear mixed models and data plotting, respectively.

# 3 | RESULTS

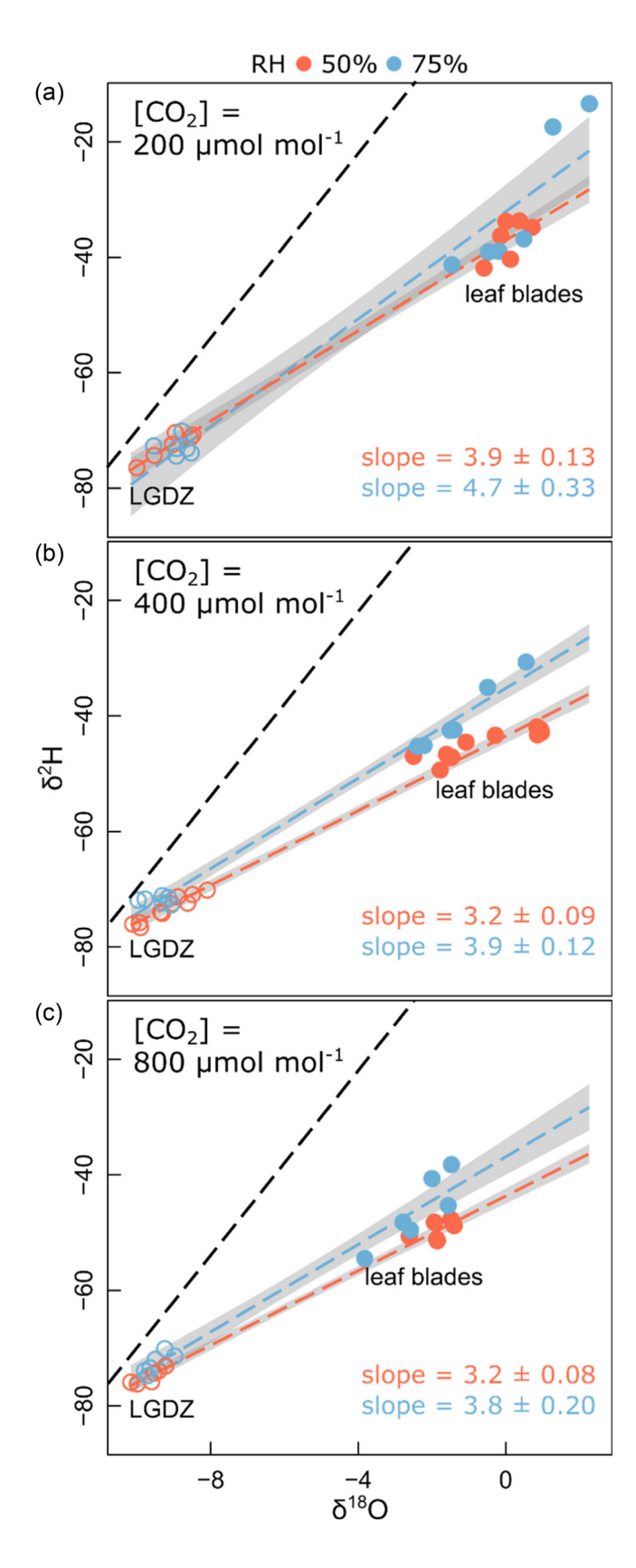
# 3.1 | $^{18}$ O enrichment of bulk leaf water ( $\Delta^{18}$ O<sub>LW</sub>), photosynthetic tissue water ( $\Delta^{18}$ O<sub>SSW</sub>), evaporative site enrichment ( $\Delta^{18}$ O<sub>e</sub>) and relations among them

 $\Delta^{18}O_{LW}$  determined near the end of the 16 h-long periods of constant light ranged between 7.9% and 10.2% and responded significantly to [CO<sub>2</sub>], with the increase of [CO<sub>2</sub>] from 200 to

.3653040, 2023, 9, Downloaded from https:

Jülich GmbH Research Center, Wiley Online Library on [25/08/2023]. See the Term

 $800\,\mu mol\,mol^{-1}$  causing decreases of  $\Delta^{18}O_{LW}$  of 1.3% at a daytime RH of 50% (designated 'low RH' in the following) and 2.3‰ at a daytime RH of 75% ('high RH') (Table 2, Supporting Information: Figure S2). RH alone and the interaction of RH and [CO2] had no



significant effects on  $\Delta^{18}O_{LW}$ . Similar treatment effects (or their absence) were detected for  $\Delta^{18}O_{LW}$  near the end of the dark period. However,  $\Delta^{18}O_{LW}$  changed slightly more between the end of the light and the end of the dark period in the low than the high RH treatment, likely owing to the fact that the low RH treatment involved a 25%-increase of RH between the light and dark periods, while RH was kept constant in the high RH treatment. Overall, however, the changes of  $\Delta^{18}O_{LW}$  between the end of the light and the end of the dark period were small ( $\sim 1.6\%$  at low RH and  $\sim 0.8\%$ at high RH). These effects were consistent in replicated (n = 3-5) mesocosm-scale experiments. Although the absence of a significant daytime-RH effect on  $\Delta^{18}O_{LW}$  was unexpected, plots of  $\delta^{18}O$  versus δ<sup>2</sup>H-made using end-of-the-light-period leaf water and leaf growth zone samples-demonstrated a significantly steeper slope (Figure 1) and a lower deuterium deviation with reference to the global meteoric water line (Supporting Information: Table S2) for the high RH compared with the low RH treatment, for all [CO<sub>2</sub>] levels, supporting a differential effect of daytime evaporative conditions on bulk leaf water isotope composition (Voelker et al., 2014) (see also discussion under Section 4.4).

The  $^{18}\text{O}$  enrichment of photosynthetic medium water ( $\Delta^{18}\text{O}_{\text{SSW}}$ ) was calculated as  $\Delta^{18}\text{O}_{\text{Sucrose}}$  –  $\epsilon_{\text{bio}}$  (with  $\epsilon_{\text{bio}}$  constant at 26.7%; see Section 2.7).  $\Delta^{18}\text{O}_{\text{Sucrose}}$  did not differ between samples collected between the end of the light and end of the dark period (Supporting Information: Table S1).  $\Delta^{18}\text{O}_{\text{SSW}}$  responded to both RH and [CO2] treatments, with no significant interaction between RH and [CO2] (Table 2, Supporting Information: Figure S2). That is, the RH response was the same for all CO2 treatments. In all treatments,  $\Delta^{18}\text{O}_{\text{SSW}}$  was more enriched than  $\Delta^{18}\text{O}_{\text{LW}}$ , and this enrichment was much greater at low RH (+7.4 to +8.7%) than at high RH (+2.2 to +2.4%). At the same time,  $\Delta^{18}\text{O}_{\text{SSW}}$  decreased by ~2.4% between 200 and 800 µmol mol $^{-1}$  CO2. The average RH and [CO2] sensitivities of  $\Delta^{18}\text{O}_{\text{SSW}}$  were ~0.24%/% and ~0.004%/µmol mol $^{-1}$ .

Craig–Gordon modelled evaporative site enrichment ( $\Delta^{18}O_e$ ) also responded significantly to RH and [CO $_2$ ] (Table 2). However, the [CO $_2$ ] effect on  $\Delta^{18}O_e$  was opposite to that for  $\Delta^{18}O_{SSW}$ , as  $\Delta^{18}O_e$  increased (by 2.1‰ at low RH and 2.8‰ at high RH) when [CO $_2$ ] during growth was increased from 200 to 800 µmol mol $^{-1}$ . The

**FIGURE 1** Isotopic composition of leaf blade water (closed symbols) and water in the leaf growth-and-differentiation zone (LGDZ) (open symbols) in  $\delta^2 H - \delta^{18} O$  dual isotope space at two daytime relative air humidity levels (RH): 50% (red) and 75% (blue) at three atmospheric CO<sub>2</sub> concentrations during plant growth: 200 (a), 400 (b) and 800 μmol mol<sup>-1</sup> (c). The blue and red dashed lines and the shadowed areas indicate the evaporation lines ± confidence interval (CI) 95% for the different treatments. The black dashed line indicates the global meteoric water line ( $\delta^2 H = 10\% + 8 \times \delta^{18} O$ ). Data points correspond to individual samples taken near the end of the light period in replicated (n = 3-5) mesocosm-scale experiments of *Lolium perenne*. For all individual CO<sub>2</sub> levels, the slope was higher at high daytime RH compared to low daytime RH (slope values ± SE are presented inside the panels).

Plant, Cell & Environment

PC-WILEY 2637

average RH and  $CO_2$  sensitivities of  $\Delta^{18}O_e$  were -0.28%/% and  $+0.004\%/\mu\text{mol mol}^{-1}$ .

 $\Delta^{18} O_{SSW}$  was significantly related to  $\Delta^{18} O_e$  ( $R^2$  = 0.69, p = 0.04), but not to  $\Delta^{18} O_{LW}$  ( $R^2$  = 0.20, p = 0.38) if all treatments were pooled (Figure 2). Nevertheless, there were treatment-specific differences between  $\Delta^{18} O_{SSW}$  and  $\Delta^{18} O_e$ . While  $\Delta^{18} O_{SSW}$  was similar to  $\Delta^{18} O_e$  at ambient [CO<sub>2</sub>],  $\Delta^{18} O_{SSW}$  was higher than  $\Delta^{18} O_e$  at low [CO<sub>2</sub>] and lower at high [CO<sub>2</sub>]. This [CO<sub>2</sub>] effect on  $\Delta^{18} O_{SSW} - \Delta^{18} O_e$  was very similar in the two RH treatments (Figure 2b).

The proportional difference between  $\Delta^{18}O_{LW}$  and  $\Delta^{18}O_{e}$  ( $\phi_{LW}=1-\Delta^{18}O_{LW}/\Delta^{18}O_{e}$ ) varied between 0.03 and 0.57, and was influenced by RH and [CO<sub>2</sub>], as well as their interaction (Table 2).  $\phi_{LW}$  was higher at low RH than at high RH at every [CO<sub>2</sub>] and increased with [CO<sub>2</sub>], with this [CO<sub>2</sub>]-driven effect being much higher at high RH. Conversely, the proportional difference between photosynthetic tissue water and evaporative site <sup>18</sup>O enrichment ( $\phi_{SSW}$ ) was smaller (–0.17 to 0.23) and did not respond to RH, but increasing [CO<sub>2</sub>] caused an increase of  $\phi_{SSW}$ .

# 3.2 Gas exchange parameters, LWC and turnover

Leaf measurements of stomatal conductance for water vapour  $(g_{s H_2O})$ and transpiration (E<sub>leaf</sub>) of paired plants were performed under conditions approximating those in the growth environment in each experimental run (Table 2) and have been reported by Baca Cabrera et al. (2020). Briefly,  $g_{s H_2O}$  responded significantly to  $[CO_2]$  and RH and their interaction. Specifically,  $g_{s \; H_2O}$  decreased exponentially with [CO2] with an RH-sensitivity that decreased with [CO2]. In the low [CO<sub>2</sub>] treatment,  $g_{s H_2O}$  was 2.6-fold greater at high than at low RH, but only 1.5-fold greater at high [CO<sub>2</sub>]). E<sub>leaf</sub> also decreased exponentially (by ~62%) with increasing [CO<sub>2</sub>] and was higher at low than at high RH (+12%, +22% and +45% at low, ambient and high [CO<sub>2</sub>]). Notably, the  $g_{s H_2O}$  to  $E_{leaf}$  ratio decreased with [CO<sub>2</sub>]. This effect was (at least partially) related to systematic differences in air temperature among treatments (up to 1.3°C), caused by differences in E<sub>leaf</sub> (leaf temperature was fixed at 21°C), associated offsets between leaf and air temperature (up to 0.9°C) (Figure 3) and offsets of actual relative to nominal %RH conditions (up to 3% RH) during gas exchange measurements in the leaf cuvette. We also observed systematic differences among treatments in the average canopy temperature (as measured with thermocouples; range 19.1-21.0°C), which were inversely related to canopy scale transpiration (Baca Cabrera et al., 2020). This indicates that the results observed at the leaf cuvette level were essentially also reflected at the entire sward scale.

Mesophyll conductance  $(g_m)$  decreased near-linearly by ~54% between low and high [CO<sub>2</sub>] and was ~26% smaller at high than at low RH (Table 2). Also,  $g_m$  correlated linearly with  $E_{leaf}$  ( $R^2$  = 0.89), but the correlation between  $g_m$  and  $g_s$  was not significant.

LWC was practically the same in the different treatments (12.2–12.9  $\rm mol\,m^{-2}$ ), except at high [CO $_2$ ]/low RH, where LWC was 11% higher than the average of the other treatments (Table 2). Accordingly, the turnover time of bulk leaf water (calculated as LWC/

 $E_{\rm leaf}$ ) was primarily determined by the variation of  $E_{\rm leaf}$  and varied between 62 min (low [CO<sub>2</sub>] and low RH) and 212 min (high [CO<sub>2</sub>] and high RH).

# 3.3 | <sup>18</sup>O enrichment of nonphotosynthetic tissue water

<sup>18</sup>O enrichment of the nonphotosynthetic leaf water fraction  $(\Delta^{18}O_{non-SSW})$  was first estimated by Equation 15 using a  $f_{non-SSW}$ SSW = 0.53, the anatomically based estimate of the nonmesophyll water fraction in the bulk leaf (Figure 4a, left panel). The proportional offset of  $\Delta^{18}O_{non-SSW}$  from  $\Delta^{18}O_{e}$  ( $\phi_{non-SSW}$  $_{SSW} = 1 - \Delta^{18}O_{non-SSW}/\Delta^{18}O_e$ ) is given in Figure 4b (left panel). The estimates of  $\Delta^{18}O_{non-SSW}$  thus obtained relied on the assumption that the mesophyll was well-mixed (as explained in Section 2.7, and consistent with Equation 7), which implied that  $\Delta^{18}O_{SSW}$  was representative for the entire mesophyll, including the mesophyll vacuoles. Under this assumption,  $\Delta^{18}O_{non-SSW}$  was 2.0% on average for the low RH treatments, implying that the  $\delta^{18}\text{O}$  of water in the non-SSW fraction was relatively close to source water (specifically, decreasing  $f_{non-SSW}$  below 0.48 predicted negative  $\Delta^{18}O_{non-SSW}$  for these treatments). Conversely, at high RH, isotopic mass balance (Equation 15) indicated that the nonphotosynthetic leaf water fraction was distinctly <sup>18</sup>O enriched, and particularly so at low [CO<sub>2</sub>] (+8.3%).

Increasing  $f_{\text{non-SSW}}$  from 0.53 to 0.88—which considered non-perfect mixing of the mesophyll, that is, an increasing proportion of the mesophyll having the same  $\Delta^{18}\text{O}$  as the nonmesophyll tissue—predicted increases of  $\Delta^{18}\text{O}_{\text{non-SSW}}$  (Figure 4a) and corresponding decreases of  $\phi_{\text{non-SSW}}$  in all treatments (Figure 4b). This effect was most apparent at low RH. That is, with the type of sensitivity analysis used here, consideration of nonperfect mixing of the mesophyll was associated with a much smaller effect on estimates of  $\Delta^{18}\text{O}_{\text{non-SSW}}$  at low RH than at high RH.

# 3.4 | Relationships between gas exchange parameters and <sup>18</sup>O enrichment of whole-leaf water, and of the photosynthetic and nonphotosynthetic tissue water fractions

Overall, the relationship between  $E_{leaf}$  and  $\phi_{LW}$  was nonsignificant ( $R^2$  = 0.14; p > 0.05) and exhibited great scatter (Figure 5a). However, this scatter hid systematic, but opposing RH and [CO<sub>2</sub>] effects on the relationship between  $E_{leaf}$  and  $\phi_{LW}$ : an RH-driven positive relationship evident at each individual [CO<sub>2</sub>] level, and a counteracting negative relationship driven by variation of [CO<sub>2</sub>], which was present at both RH levels. Meanwhile,  $E_{leaf}$  and  $\phi_{SSW}$  (calculated as  $\phi_{SSW}$  = 1 –  $\Delta^{18}O_{SSW}/\Delta^{18}O_e$ ) correlated negatively across the treatments ( $R^2$  = 0.81; p < 0.05) (Figure 5b). Conversely, the relationship between  $E_{leaf}$  and  $\phi_{non-SSW}$  (calculated as  $\phi_{SSW}$  = 1 –  $\Delta^{18}O_{non-SSW}/\Delta^{18}O_e$ ) was nonsignificant irrespective of the

3653040, 2023, 9, Downloaded from https

, Wiley Online Library

on Wiley Online Library for rules of use; OA articles are governed by the

value at which  $f_{\text{non-SSW}}$  was fixed (Figure 5c for  $f_{\text{non-SSW}}$  = 0.53; data for other values of  $f_{\text{non-SSW}}$  not shown). Also,  $\phi_{\text{non-SSW}}$  displayed qualitatively similar treatment-dependent relationships with  $E_{\text{leaf}}$  as  $\phi_{\text{LW}}$  (compare Figure 5a,c).

 $\phi_{SSW}$  was negatively correlated with  $g_{s\ CO_2}$ ,  $g_m$  and total conductance ( $g_{total}$ , calculated as  $1/(1/g_{s\ CO_2}+1/g_m)$ ) (Figure 6). The correlation between  $\phi_{SSW}$  and  $g_{total}$  was particularly strong ( $R^2$  = 0.93; p < 0.01), while the one with  $g_{s\ CO_2}$  alone ( $R^2$  = 0.79; p = 0.02) appeared to vary between RH levels. The correlation of  $\phi_{SSW}$  with  $g_m$  was only marginally significant ( $R^2$  = 0.62; p = 0.06). In contrast,  $\phi_{LW}$  and  $\phi_{non-SSW}$  did not correlate with  $g_m$  (not shown), similar to the relationships with  $E_{leaf}$ , which were also nonsignificant (compare with Figure 5a.c).

 $\phi_{\text{non-SSW}}$  demonstrated a very close, saturating relationship with the ratio of  $E_{\text{leaf}}$  to water vapour influx, estimated as  $g_{s \text{ H}_2\text{O}} \times w_a$  (Pseudo- $R^2$  = 0.99, p < 0.05 for fixed  $f_{\text{non-SSW}}$  of 0.53) (Figure 7). Increasing  $f_{\text{non-SSW}}$  from 0.53 to 0.70 or 0.88 did not alter this relationship in a qualitative sense (Pseudo- $R^2$  = 0.98 and 0.96, respectively), although it did change the value of the asymptote. Similar, although more blurred relationships existed between  $\phi_{\text{LW}}$  and the ratio of  $E_{\text{leaf}}$  to water vapour influx (not shown). Conversely, there was no significant relationship (p > 0.05) between  $\phi_{\text{SSW}}$  and the ratio of  $E_{\text{leaf}}$  to water vapour influx.

Using the data presented in Table 2 to fit the Péclet model as presented in Equation 7, we obtained estimates of the effective path length (termed  $L_{CG}$ ) for the different treatments (Figure 4c). These estimates of L were sensitive to (i) the assumptions of  $f_{non-SSW}$  used in the estimation of  $\Delta^{18}O_{non-SSW}$ , and growth conditions of (ii) [CO<sub>2</sub>] and (iii) daytime RH (Figure 4c). In general, however, L increased with increasing  $[CO_2]$  and decreased with daytime RH. Specifically, at  $f_{non-}$ SSW = 0.53, L increased from 63 to 132 mm between low and ambient [CO<sub>2</sub>] (no value could be fitted for the high [CO<sub>2</sub>] level) at 50% RH and from 4 to 182 mm between high and low [CO<sub>2</sub>] at 75% RH. Alternatively, we also estimated L (termed  $L_{SSW}$ , Figure 4d) using the same data, except for replacing  $\Delta^{18}O_e$  by  $\Delta^{18}O_{SSW}$ , the  $\Delta^{18}O$  of the photosynthetic water pool, which is represented by the first term on the right-hand side of Equation 7. This yielded qualitatively similar estimates of L, except that the effect of  $[CO_2]$  on L was attenuated. Thus, estimates of  $L_{SSW}$  were higher than  $L_{CG}$  at low  $[CO_2]$ , but lower at high [CO<sub>2</sub>].

# 4 | DISCUSSION

# 4.1 | On the approach—Advances and caution

Here, we present a new type of compartmental analysis of bulk leaf water  $^{18}\text{O}$  enrichment ( $\Delta^{18}\text{O}_\text{LW}$ ), based on the propositions of Holloway-Phillips et al. (2016) (see their eqns. 9–11). This analysis distinguished  $\Delta^{18}\text{O}$  in the photosynthetic tissue ( $\Delta^{18}\text{O}_\text{SSW}$ ) and nonphotosynthetic tissue ( $\Delta^{18}\text{O}_\text{non-SSW}$ ) by using an isotopic mass balance (Equation 6) and estimates of the bulk leaf water fractions in photosynthetic and nonphotosynthetic leaf tissues, where the latter includes the veins and epidermis. This analysis

rested partly, but significantly, on published comprehensive leaf anatomical analyses of C<sub>3</sub> grasses (Dengler et al., 1994), including L. perenne (Charles-Edwards et al., 1974), the object of this work. This approach is functionally distinct and alternative to previous works which divided bulk leaf water into leaf lamina and primary vein water (see Section 1, Gan et al., 2002, 2003; Yakir et al., 1994) particularly for how water in the epidermis (a co-dominant component of bulk leaf water) is attributed to the functional parts of the leaf: exclusively associated with the nonphotosynthetic leaf tissue (which also includes the veins) in the present approach; and mostly with the lamina fraction (which includes the photosynthetic tissue) when the bulk leaf is separated in its lamina and (main) vein parts, in the earlier approach. Likewise, consistent with the proposition of Holloway-Phillips et al. (2016), we argue that the photosynthetic tissue was in (or near) equilibrium with <sup>18</sup>O-enrichment at the evaporative sites as predicted by the Craig-Gordon model (although small offsets were systematic; see discussion under Section 4.2). Conversely, the nonphotosynthetic tissue, including vascular tissue and epidermis, appeared to display a treatment-dependent Péclet effect (Section 4.2).

However, the present analysis relied on several assumptions, including (1) that  $\epsilon_{bio}$  for sucrose was the same (26.7‰) in all treatments, meaning that there was a constant offset between  $\Delta^{18}O_{Sucrose}$  and  $\Delta^{18}O_{SSW}$  across treatments. Assumptions specifically important for the analysis of nonphotosynthetic tissue water fraction were more numerous and required, for all treatments, that (2) the mesophyll was well-mixed, (3)  $f_{non\text{-}SSW}$  was 0.53, (4) the ratio of assimilation to transpiration (A/E) was constant over the leaf surface and (5) that Equation 7, which was used to calculate L in the nonphotosynthetic tissue water fraction, provides a reasonable description of  $\Delta^{18}O_{LW}$ . Considering uncertainty, however, we did relax specific assumptions of the analysis, as we discuss below.

Concerning (1): the temperature-dependent (Hirl et al., 2021; Sternberg & Ellsworth, 2011)  $\varepsilon_{bio}$  chosen here was very close to the 'constant 27‰' assumption which has been used most commonly (Barbour, 2007; Cernusak et al., 2005; Lehmann et al., 2017) as we used a thermal environment for which the  $\varepsilon_{bio}$  estimates of the two approaches converged closely (air temperature in the light period = 20°C). This estimate of  $\varepsilon_{bio}$  is taken from that for cellulose formation (Barbour, 2007; Cernusak et al., 2003); we are not aware of independent confirmations of  $\varepsilon_{bio}$  for sucrose in photosynthesizing leaves. Importantly, however, we found no evidence for incomplete equilibration of carbonyl groups with sucrose synthesis water, as the  $\delta^{18}$ O of sucrose did not differ significantly between plants grown in the presence of  $\epsilon^{18}$ O-enriched or  $\epsilon^{18}$ O-depleted CO<sub>2</sub> (Supporting Information: Figure S3), similarly to cellulose (Liu et al., 2016). Also, the  $\delta^{18}$ O of bulk leaf water was not affected by the  $\epsilon^{18}$ O of CO<sub>2</sub> ( $\epsilon^{18}$ O of CO<sub>2</sub> ( $\epsilon^{18}$ O of D-0.)

Further, (2):  $\Delta^{18}O_{\text{Sucrose}}$  did not vary between the end of the light period and the end of the dark period, indicating that diurnal variation in mobilization of sucrose from the vacuole or recycling of sucrose via hydrolysis or fructan metabolism (Lattanzi et al., 2012; Pollock & Cairns, 1991) did not alter the  $^{18}O$  composition of sucrose. The apparent constancy of  $\Delta^{18}O_{\text{Sucrose}}$  could be related to a relative constancy of  $\Delta^{18}O$  of mesophyll water, as we observed only very small (if any) variation of  $\Delta^{18}O_{\text{LW}}$  between the end of the day and

**TABLE 2** Effect of atmospheric CO<sub>2</sub> concentration and daytime RH and their interaction on <sup>18</sup>O enrichment ( $\Delta^{18}$ O) of bulk leaf water sampled at ~2 h before the end of the 16 h-long light ( $\Delta^{18}$ O<sub>LW day</sub>) and 8 h-long dark periods ( $\Delta^{18}$ O<sub>LW night</sub>), sucrose synthesis water ( $\Delta^{18}$ O<sub>SSW</sub>), modelled leaf-level evaporative site <sup>18</sup>O enrichment during the light period ( $\Delta^{18}$ O<sub>e</sub>), proportional deviation between  $\Delta^{18}$ O<sub>LW day</sub> and  $\Delta^{18}$ O<sub>e</sub> ( $\phi_{SSW}$ ), physiological parameters of *Lolium perenne* leaves: transpiration ( $E_{leaf}$ ), stomatal conductance to water vapour ( $g_{S H_2O}$ ) and mesophyll conductance ( $g_m$ ), LWC and leaf water turnover time (calculated as LWC/ $E_{leaf}$ ).

_	Daytime RH (%)								
	50	,70)		75					
	Atmospheric CO <sub>2</sub> concentration (μmol n						Effect significance (p value)		
Parameter	200	400	800	200	400	800	CO <sub>2</sub>	RH	CO <sub>2</sub> :RH
$\Delta^{18} O_{LW~day}~(\%)$	9.9 (0.2)	9.6 (0.5)	8.6 (0.2)	10.2 (0.9)	9.2 (0.8)	7.9 (0.4)	<0.01	0.55	0.47
$\Delta^{18}O_{LW\ night}$ (%)	8.5 (0.3)	8.2 (0.1)	6.7 (0.4)	8.8 (0.6)	8.6 (0.1)	7.6 (0.5)	<0.001	0.09	0.34
$\Delta^{18} O_{SSW}$ (‰)	18.7 (1.9)	17.5 (0.7)	15.9 (0.8)	12.4 (0.5)	11.3 (1.0)	10.3 (0.2)	0.02	<0.001	0.74
Δ <sup>18</sup> O <sub>e</sub> (‰)	18.0 (0.2)	19.0 (0.1)	20.1 (0.2)	10.6 (0.4)	12.3 (0.3)	13.4 (0.1)	<0.001	<0.001	0.19
$\phi_{LW}$	0.45 (0.01)	0.50 (0.02)	0.57 (0.01)	0.03 (0.11)	0.26 (0.06)	0.41 (0.03)	<0.001	<0.001	0.03
Φssw	-0.04 (0.12)	0.08 (0.04)	0.20 (0.05)	-0.17 (0.05)	0.08 (0.06)	0.23 (0.01)	<0.001	0.54	0.26
$E_{\text{leaf}}$ (mmol m <sup>-2</sup> s <sup>-1</sup> )	3.3 (0.3)	2.3 (0.2)	1.4 (0.1)	2.9 (0.2)	1.9 (0.2)	1.0 (0.1)	<0.001	0.01	0.64
$g_{\rm s \ H_2O} \ ({\rm mol \ m^{-2} \ s^{-1}})$	0.30 (0.03)	0.19 (0.02)	0.11 (0.01)	0.78 (0.08)	0.35 (0.04)	0.16 (0.03)	<0.001	<0.001	<0.001
$g_{\rm m} \ ({\rm mol} \ {\rm m}^{-2} \ {\rm s}^{-1})$	0.43 (0.04)	0.37 (0.07)	0.22 (0.05)	0.36 (0.02)	0.31 (0.03)	0.14 (0.02)	<0.001	0.06	0.81
LWC (mol m <sup>-2</sup> )	12.2 (0.1)	12.9 (0.2)	13.8 (0.2)	12.8 (0.0)	12.2 (0.1)	12.4 (0.0)	<0.01	<0.01	<0.001
Turnover time (min)	62 (1)	92 (1)	163 (2)	73 (0)	107 (1)	212 (1)	<0.001	<0.001	<0.001

Note: Averages for each treatment (mean  $\pm$  SE) and p values of a two-way ANOVA for multiple physiological parameters measured in replicated mesocosm experiments. Significant effects are given in bold type. Averages were calculated based on individual leaf replicates in the case of gas exchange parameters ( $E_{\text{leaf}}$ ,  $g_{\text{S}}$  H<sub>2</sub>O and  $g_{\text{m}}$ , n = 6–12) and canopy scale replicates for all other parameters (n = 3–5).

Abbreviations: ANOVA, analysis of variance; LW, leaf water; LWC, leaf water content; RH, relative humidity; SSW, sucrose synthesis water.

end of the night. Conversely, however, Lehmann et al. (2017) found that hexoses were depleted by ~2\% relative to sucrose, equivalent to a ~2‰ depletion of the synthesis water of hexoses relative to sucrose, if the  $\varepsilon_{bio}$  was the same for both sugars. This could indicate that metabolism of hexoses derived from sucrose was associated with significant oxygen exchange in a less <sup>18</sup>O-enriched environment locally, or that the hexose-to-sucrose ratio varied along the leaf in parallel with <sup>18</sup>O enrichment of medium water (Lehmann et al., 2017). Evidence for a different subcellular localization was presented by Wagner et al. (1983) who found hexoses to be virtually exclusively localized in the vacuole and a significant fraction of the sucrose in the cytosol of mesophyll cells isolated from barley primary leaves. Most interestingly, Koroleva et al. (1998) found a much higher hexose-tosucrose ratio in epidermal cells of barley leaves than in the mesophyll (or bundle sheath parenchyma). If epidermis water is less <sup>18</sup>O enriched than mesophyll water (as we suggest), this could also explain a lesser <sup>18</sup>O enrichment of hexoses in whole-leaf extracts.

Nevertheless, we realize that direct empirical proof for the (eventual) constancy (or absence thereof) of  $\epsilon_{bio}$  for leaf sucrose ( $\epsilon_{bio}$   $_{Sucrose}$ ) is presently missing. Certainly, there is a critical need for experimental determinations across a range of plant functional groups, environmental conditions and diurnal cycles (Holloway–Phillips et al. 2022). This includes possible metabolically based variation of  $\epsilon_{bio}$   $_{Sucrose}$  (a) at the site of primary synthesis in the mesophyll, (b) during transport to and into sieve elements, and (c) in

association with sucrose-consumption and resynthesis during eventual storage along the path in nonphotosynthetic leaf tissue.

Although we did not perform anatomical investigations ourselves, we believe that assumption (3) was well-founded for a  $f_{non-SSW} = 0.53$ , if the mesophyll was well-mixed. Estimates of mesophyll and nonmesophyll proportions of C<sub>3</sub> grass leaves are known to vary comparatively little among and within studies (e.g., Charles-Edwards et al., 1974; Dengler et al., 1994; Garnier & Laurent, 1994; Winter et al., 1993). In particular, fractions of mesophyll and nonmesophyll tissue observed by Charles-Edwards et al. (1974) were remarkably constant among genotypes of L. perenne across contrasting growth conditions. Although leaf thickness correlated with the proportion of mesophyll, this parameter displayed little variation across diverse environments (Charles-Edwards et al., 1974). Also, we found very little variation of leaf thickness, based on LWC (Table 2). Moreover, leaf length and width, and epidermal cell number and length did not differ between treatments (Baca Cabrera et al., 2020). Finally, a minimum  $f_{\text{non-SSW}} \sim 0.5$  was also supported by isotopic mass balance (Equation 15). Thus, we propose as the most parsimonious hypothesis that the proportions of mesophyll (and nonmesophyll) tissue, and hence  $f_{SSW}$  (and  $f_{non-SSW}$ ) were very closely similar between the different growth environments.

Assumption (4) is predicted by optimal stomatal control theory (Cowan & Farquhar, 1977) and supported by the close agreement between  $\Delta^{18} O_e$  and  $\Delta^{18} O_{SSW}$  for the ambient [CO $_2$ ] treatments at both high and low RH. Yet, we did observe small but systematic

3653040, 2023, 9, Downloaded

GmbH Research Center, Wiley Online Library on [25/08/2023]. See the Terms

) on Wiley Online Library for rules of use; OA articles are governed by the applicable Creative Commons

**FIGURE 2** Relationship between  $\Delta^{18}$ O of leaf water ( $\Delta^{18}$ O<sub>LW</sub>) and  $\Delta^{18}$ O of photosynthetic medium water ( $\Delta^{18}$ O<sub>SSW</sub>) (a) and between leaf-scale  $\Delta^{18}$ O at the evaporative sites, calculated with the Craig–Gordon model ( $\Delta^{18}$ O<sub>e</sub>), and  $\Delta^{18}$ O<sub>SSW</sub> (b) in young fully-expanded leaf blades of *Lolium perenne* plants grown in stands at different atmospheric CO<sub>2</sub> concentrations (circles, 200; triangles, 400; squares, 800 µmol mol<sup>-1</sup>), at low (RH = 50%, red symbols) and high daytime (RH = 75%, blue symbols). The dashed line represents the regression line of the relationship (only shown when significant, p < 0.05). The continuous line represents the 1:1 line. Data points and error bars represent the mean ± SE. RH, relative humidity. [Color figure can be viewed at wileyonlinelibrary.com]

 $[\text{CO}_2]$ -dependent variation of  $\phi_{\text{SSW}}$  (range -0.17 to +0.23), as we discuss below.

# 4.2 | <sup>18</sup>O enrichment of sucrose more closely related to evaporative site enrichment than to whole-leaf water

Our work confirms the observation of Lehmann et al. (2017) of a significant and RH-dependent underestimation of  $\Delta^{18}O_{Sucrose}$  by  $\Delta^{18}O_{LW}+\epsilon_{bio}$  (26.7%) in *L. perenne*. In fact, the underestimation observed at low daytime RH was higher than that observed by Lehmann et al. (2017). Thus, the RH sensitivity of  $\Delta^{18}O_{Sucrose}$  (–0.24%-/%) was markedly greater at every [CO<sub>2</sub>] level than the RH sensitivity estimated for their data (ca. –0.16%-/% on average of the two grasses).

Additionally, our data reveal an overall closer agreement of  $\Delta^{18} O_{SSW}$  (i.e.,  $\Delta^{18} O_{Sucrose}$  –  $\epsilon_{bio}$ ) with  $\Delta^{18} O_{e}$  than with  $\Delta^{18} O_{LW}$ . This result differs from the conclusion of Cernusak et al. (2003) which was based on the comparison of the  $^{18} O$  enrichment of phloem dry matter (mostly sucrose; e.g., Smith & Milburn, 1980) with lamina water (which excluded the main veins) or  $\Delta^{18} O_{e}$  in a dicot (*R. communis*). However, as our analysis was based on bulk leaf water, it is not strictly comparable with that of Cernusak et al. (2003). As shown by Gan et al. (2003) and Barbour et al. (2021), accounting for the vein fraction—which represents by itself only a fraction of the total nonphotosynthetic tissue water (see above)—already reduces substantially the discrepancy between  $^{18} O$  enrichment of lamina water and  $\Delta^{18} O_{e}$ . Unfortunately, sufficiently-rapid, artifact-free

physical separation of the nonphotosynthetic and photosynthetic leaf tissue of *L. perenne* (or other C<sub>3</sub> grasses) appears to be practically impossible at present (see also discussions in Cernusak et al., 2003).

The offset between  $\Delta^{18}O_{SSW}$  and  $\Delta^{18}O_{e}$  was influenced strongly by [CO<sub>2</sub>], but not by RH or the interaction of [CO<sub>2</sub>] and RH. This effect correlated closely with the effect of  $[CO_2]$  on  $E_{leaf}$ ,  $g_s$ ,  $g_m$  and  $g_{total}$ . To our best knowledge, the relationship between  $\phi_{SSW}$  and gas exchange parameters has not been investigated previously, reducing opportunities for discussion. However, Ferrio et al. (2012) observed an apparent coordination between mesophyll (and hydraulic) conductance and effective path length (L) in vein-severing experiments with droughted and control plants of Vitis vinifera. Our observation of a negative relationship between  $E_{leaf}$  and  $\phi_{SSW}$  (Figure 5b) also implies a (strong) decrease of L with increasing  $E_{leaf}$ , an effect previously observed in tree species (Loucos et al., 2015; Song et al., 2013); and-since  $E_{leaf}$  and  $g_m$  (as well as  $g_{total}$ ) were closely correlated—there may have also been a negative association between  $g_m$  and L, consistent with observations of Ferrio et al. (2012), when applied only to photosynthetic medium water in the present case.

An increase in L under increasing [CO<sub>2</sub>] for both RH levels could also be related to changes in anatomical features of stomata. Studies in *Arabidopsis* (Larcher et al., 2015) and mangrove plants (Sternberg & Manganiello, 2014) indicated a decrease in L with increasing stomatal density, associated with a decrease in the distance between the stomatal pores and the veins and an increase in the total cross-sectional area through which mesophyll water flows. As [CO<sub>2</sub>] has risen, stomatal density has decreased (and pore size increased) over geological time (Franks & Beerling, 2009). A similar behaviour has been observed in controlled experiments under elevated [CO<sub>2</sub>] for a

Notably, based on our analysis,  $\Delta^{18}O_{SSW}$  was slightly greater than  $\Delta^{18}O_e$  (implying that  $\phi_{SSW}$  < 0) at low [CO<sub>2</sub>] in both RH treatments. As  $\Delta^{18}O_{SSW}$  has not been analyzed previously, there is no other work with which this observation can be compared. However, negative values of  $\phi_{LW}$  have been observed quite frequently in different plant functional groups (Cernusak et al., 2016, 2022), including in grasses (Helliker & Ehleringer, 2000), although such relationships are theoretically unexpected in steady-state conditions (Farguhar & Gan, 2003; Gan et al., 2003; Ogée et al., 2007). Because of the expectation that  $\Delta^{18} O_{SSW}$  should always be greater than  $\Delta^{18}O_{LW}$ , we would assume that such reported negative  $\phi_{LW}$  values were also associated with (even more) negative  $\phi_{\text{SSW}}$  values.

Errors in the simplifying assumptions for the calculation of  $\Delta^{18}O_e$  (i.e., absence of cuticular transpiration, stomatal patchiness and RH and temperature gradients between base and tip of the leaf and the canopy) could perhaps also contribute to a mismatch between  $\Delta^{18}O_e$  and  $\Delta^{18}O_{SSW}$ . In particular, the increase in  $\Delta^{18}O_e$  from the leaf base toward the tip, which has been observed in grasses (Helliker & Ehleringer, 2000; Ogée et al., 2007) was not included in our model. A similar increase is expected for  $\Delta^{18}O_{SSW}$  but has not been studied so far. At the same time, transpiration (E) (Helliker & Ehleringer, 2000; Ogée et al., 2007) and photosynthesis (A) (Meinzer & Saliendra 1997; Xiong et al., 2015) are known to increase from the leaf base to the

**FIGURE 3** Air temperature  $(T_{air})$  (a), difference between leaf temperature ( $T_{leaf}$ ) and  $T_{air}$  (b) and water vapour concentration gradient between the substomatal cavities (w<sub>i</sub>) and ambient air (w<sub>a</sub>) (c) during leaf gas exchange measurements of Lolium perenne leaves (youngest mature, i.e., fully-expanded, leaf blades). Plants were grown in dense canopies under contrasting CO<sub>2</sub> concentrations (circles, 200; triangles, 400; squares, 800 µmol mol<sup>-1</sup>) and daytime RH levels (low RH = 50%, red symbols; high RH = 75%, blue symbols). CO<sub>2</sub> concentration and RH of the growth environments were replicated in the leaf gas exchange measurements and  $T_{leaf}$  was kept constant at 21°C for all treatments. Data points and error bars represent the mean ± SE. RH, relative humidity. [Color figure can be viewed at wileyonlinelibrary.com]

FIGURE 4 Effect of the 'well-mixed mesophyll' assumption (represented by varying the fraction of nonphotosynthetic tissue water) on estimates of  $\Delta^{18}O$  of nonphotosynthetic tissue water ( $\Delta^{18}O_{non-SSW}$ ) (a), the fraction of unenriched water in the nonphotosynthetic tissue ( $\phi_{\text{non-SSW}}$ ) (b), and the effective path length (L) (c and d) in young fully-expanded leaf blades of Lolium perenne plants grown in stands at different atmospheric CO<sub>2</sub> concentrations at a daytime RH of 75% (blue bars) or 50% (red).  $f_{non-SSW}$  = 0.53 is the anatomically-based estimate of the proportion of nonmesophyll tissue in leaves of perennial ryegrass and assumes a well-mixed mesophyll (in accordance with Eqn 9 of Holloway-Phillips et al., 2016) in the equations used to estimate parameters in panels (a-d). Estimates  $f_{\text{non-SSW}} = 0.70$  or 0.88 account for the possibility that the mesophyll is not wellmixed and consider that half or all of the mesophyll vacuole volume is in equilibrium with nonmesophyll tissue (for further detail, see Section 2.7). L was estimated using either  $\Delta^{18} O_e \, (L_{CG}) \, \text{or} \, \Delta^{18} O_{SSW} \, (L_{SSW})$  for the isotopic composition of the photosynthetic water pool, that is, the first term on the right-hand side of Equation 7 (see Section 1). Data points and error bars represent the mean ± SE. Note that in (c) no L value could be fitted for the combination of low RH and  $f_{non-SSW} = 0.53$ , for the CO<sub>2</sub> concentration 800 μmol mol<sup>-1</sup>. RH, relative humidity. [Color figure can be viewed at wileyonlinelibrary.com]

leaf tip in grasses, and relative changes of the A/E ratio may vary along the leaf (Ocheltree et al., 2012), deviating from the constant A/E assumption. To which degree this relationship is affected by  $[CO_2]$  has not been explored but could perhaps play a

role in the spatial mismatch. Any spatial mismatch between (transpiration-weighted)  $\Delta^{18} \text{O}_e$  and (assimilation-weighted)  $\Delta^{18} \text{O}_\text{SSW}$ , with weighted maximum assimilation occurring closer to the leaf tip than transpiration (Lehmann et al., 2017), could

perhaps explain why  $\Delta^{18}O_{SSW} > \Delta^{18}O_e$  or  $\phi_{SSW} < 0$  at low  $[CO_2]$ (see also Ogée et al., 2007). In the same sense, the opposite spatial pattern could explain why  $\Delta^{18}O_{SSW} < \Delta^{18}O_e$  or  $\phi_{SSW} > 0$  at high [CO<sub>2</sub>], that is, the weighted maximum assimilation occurring further away from the leaf tip than transpiration. Also, the [CO<sub>2</sub>]dependent shifts could be connected to the fact that low [CO<sub>2</sub>] caused high  $g_s$  and  $g_m$ , while the opposite may have been the case at high [CO<sub>2</sub>]. Additionally, one may wonder, if a spatial mismatch between transpiration-weighted  $\Delta^{18}O_e$  and assimilationweighted  $\Delta^{18}O_{SSW}$  could also be associated with variation of transpiration and photosynthetic activity with depth inside the leaf. Finally, the assumption of a constant  $\epsilon_{\text{bio}}$  discussed in Section 4.1 could also play a role in the discrepancy between  $\Delta^{18} \text{O}_e$  and  $\Delta^{18} \text{O}_{\text{SSW}}$  at low and high [CO $_2$ ]. Clearly, these are important questions for future investigations.

# <sup>18</sup>O enrichment of nonphotosynthetic tissue water was sensitive to water vapour influx

Probably the greatest uncertainty in our analysis is connected with the estimation of  $\Delta^{18}O_{non-SSW}$  (and  $\phi_{non-SSW}$ ) as this was determined from the residual of Equation 6 (hence integrated virtually all uncertainties discussed above, see Equations 15) and Equation 5 depended on the adequacy of Equation 7 for estimation of L. For the latter, we believe that the (variable) discrepancy between  $\Delta^{18}O_{SSW}$ and  $\Delta^{18}O_{LW}$ , the comparatively close relationship between  $\Delta^{18}O_{SSW}$ and  $\Delta^{18}O_e$ , and the high  $\phi_{non\text{-SSW}}$  at low RH support well the model represented by Equation 7. Also, we did account for uncertainty in the assumption that the mesophyll was well mixed, by increasing the proportion  $f_{\text{non-SSW}}$  in a sensitivity analysis. All results demonstrated that estimates of L, and relationships of  $\Delta^{18}O_{non-SSW}$  and  $\phi_{non-SSW}$ with treatment effects and physiological parameters, remained the same in a qualitative sense.

FIGURE 5 Relationship between leaf transpiration ( $E_{leaf}$ ) and the fraction of unenriched source water in bulk leaf water  $(\phi_{IW})$  (a) in photosynthetic medium water  $(\phi_{SSW})$  (b) and in nonphotosynthetic tissue water (φ<sub>non-SSW</sub>) (c) in young fully-expanded leaf blades of Lolium perenne plants grown in stands at different atmospheric CO<sub>2</sub> concentrations (circles, 200; triangles, 400; squares, 800 µmol mol<sup>-1</sup>), at low (RH = 50%, red symbols) and high daytime RH (RH = 75%, blue symbols). Note the differences in the scaling of the y-axes.  $\phi_{\text{non-SSW}}$ was estimated using isotopic mass-balance as explained in Section 2.7) and assuming a well-mixed mesophyll for the estimation of the fraction of nonphotosynthetic tissue water ( $f_{non-SSW} = 0.53$ ). The dashed lines represent the regression lines of the relationships (only shown when significant, p < 0.05). Data points and error bars represent the mean ± SE. RH, relative humidity. [Color figure can be viewed at wileyonlinelibrary.com]

, Wiley Online Library on [25/08/2023]. See the

**FIGURE 6** Relationship between the proportional deviation of  $\Delta^{18}O_{SSW}$  from  $\Delta^{18}O_{e}$ ,  $\phi_{SSW}$  (= 1  $-\Delta^{18}O_{SSW}/\Delta^{18}O_{e}$ ), and leaf stomatal ( $g_{sCO_{2}}$ ) (a), mesophyll ( $g_{m}$ ) (b) and total (calculated as  $1/(1/g_{sCO_{2}} + 1/g_{m})$ ) (c) conductance to  $CO_{2}$  in young fully-expanded leaf blades of *Lolium perenne* plants grown in stands at different atmospheric  $CO_{2}$  concentrations (circles, 200; triangles, 400; squares, 800  $\mu$ mol mol<sup>-1</sup>), at low (RH = 50%, red symbols) and high daytime (RH = 75%, blue). The dashed lines represent the regression lines of the relationships. Data points and error bars represent the mean  $\pm$  SE. RH, relative humidity. [Color figure can be viewed at wileyonlinelibrary.com]

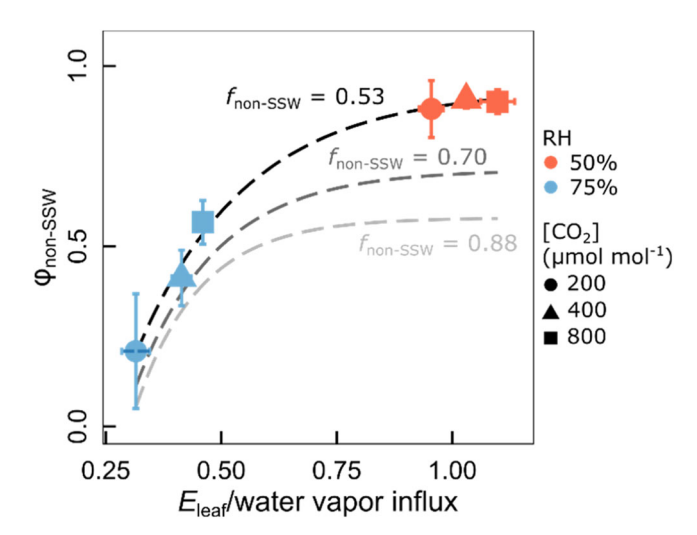


**FIGURE 7** Relationship between the ratio of transpiration ( $E_{\rm leaf}$ ) over vapour invasion (estimated as  $g_{\rm s} \times w_{\rm a}$ , Farquhar et al., 2007) and  $\phi_{\rm non-SSW}$  (the proportional deviation of  $\Delta^{\rm 18}O_{\rm non-SSW}$  from  $\Delta^{\rm 18}O_{\rm e}$ ) in young fully-expanded leaf blades of *Lolium perenne* plants grown in stands at different atmospheric CO<sub>2</sub> concentrations: 200 (circles), 400 (triangles) or 800 μmol mol <sup>-1</sup> (squares) at a daytime RH of air of 50% (red) or 75% (blue). Note that the CO<sub>2</sub>-dependent variation of  $E_{\rm leaf}$ /vapour invasion is driven by differences of  $T_{\rm leaf}$  –  $T_{\rm air}$  (see Figure 3). The dashed lines represent fitted asymptotic curves for the relationship for different  $f_{\rm non-SSW}$  values (Pseudo- $R^2$  > 0.96 in all cases). Data points and error bars represent the mean ± SE of values calculated with  $f_{\rm non-SSW}$  = 0.53 ( $f_{\rm non-SSW}$  under the assumption of a well-mixed mesophyll). RH, relative humidity. [Color figure can be viewed at wileyonlinelibrary.com]

In their analysis of the relative contributions of vapour and liquid water transport from the veins toward the stomata, Rockwell et al. (2014) predicted that an increase in  $E_{leaf}$  due to a decrease in ambient vapour mole fraction ( $w_a$ ) would pull the distribution of leaf

internal evaporation away from the perivascular space toward the stomata. Such an effect should drive an increase of L (Barbour et al., 2017). This expectation is consistent with the RH effect on L of the non-SSW leaf water fraction as estimated here, either by Equation 7 (Figure 4c) or by using a modified Equation 7, in which  $\Delta^{18}O_{\rm e}$  was replaced by  $\Delta^{18}O_{\rm SSW}$  in the first term on the right-hand side of the equation (Figure 4d). In both cases, the increase of L resulting from the decrease of RH in the growth environment was strong at every [CO $_{\rm 2}$ ] level and for every  $f_{\rm non-SSW}$  used in the estimation of  $\Delta^{18}O_{\rm non-SSW}$ .

At the same time, L increased pronouncedly with increasing [CO<sub>2</sub>] in the growth environment. This effect was associated with a decrease in E<sub>leaf</sub>, at both RH levels, independently of assumptions of  $f_{\text{non-SSW}}$ . Although Rockwell et al. (2014) did not explore effects of different [CO<sub>2</sub>] levels, this result is consistent with pulling the (evaporation-weighted) site of transpiration toward the periveinal/ perivascular space when [CO2] is decreased. The leaf gas exchange measurements-performed under environmental conditions approximating those of the growth environment-indicated a very strong  $[CO_2]$  effect on  $g_{s H_2O}$  which entrained a parallel effect on  $E_{leaf}$ , the temperature gradient between leaf  $(T_1)$  and air  $(T_2)$ ,  $T_1 - T_2$ , and hence  $w_i - w_a$  inside the leaf cuvette at both RH levels (Figure 3). Clearly, [CO<sub>2</sub>] must have had very strong effects on the energy balance of leaves, increasing the ratio of sensible to latent heat transfer, a situation that would cause an increase in the fraction of peristomatal evaporation (Rockwell et al., 2014). Again, this interpretation is consistent with our estimates of L increasing with [CO<sub>2</sub>]. The values of L (termed  $L_{CG}$ ) based on Equation 7 cover a wide range (2–182 mm for a  $f_{\text{non-SSW}}$  0.53). The range of L estimated with  $\Delta^{18}O_{e}$  replaced by  $\Delta^{18}O_{SSW}$  (termed  $L_{SSW}$ ) was distinctly smaller (by about half) but displayed qualitatively the same treatment response. Interestingly, the ranges of L estimated here are similar in magnitude to the ones

obtained for whole leaves of another  $C_3$  grass (wheat) based on anatomical investigations and a range of scenarios concerning the site of evaporation within leaves (Barbour & Farquhar, 2004; Barbour et al., 2017).

An intriguing observation made here concerns the (saturating) relationship between  $\phi_{non-SSW}$  and the ratio of  $E_{leaf}$  to water vapour influx (Figure 7). An analogous asymptotic relationship was not observed for  $\varphi_{SSW}$  but existed also for  $\varphi_{LW}$  (Pseudo- $R^2$  = 0.94), although the latter comprised more scatter due to the inclusion of the photosynthetic medium fraction in whole-leaf water.  $E_{leaf}$  equals source water influx into the leaf in the steady state, which very likely existed at the time of sampling (~14 h into the light period under constant environmental conditions, including irradiance). The ratio of  $E_{\text{leaf}}$  to water vapour influx abbreviates to  $(w_i - w_a)/w_a$  when  $g_{s H_2O}$  is eliminated from both the numerator and denominator of the ratio. This shows that at a given RH, variation of wi resulting from the variation of leaf temperature (controlled by  $g_{s H_2O}$ ) was the main determinant of the variation of  $(w_i - w_a)$ , as  $w_a$  was kept near constant in the growth chambers. At high RH, the variation of wi drove a strong variation of  $\phi_{\text{non-SSW}}$ , with  $(w_i - w_a)/w_a$  increasing dramatically in response to increasing  $[CO_2]$  due to the increase of  $T_L$ , which was a consequence of the  $g_s$ -driven decrease in  $E_{leaf}$ . Thus, at high RH, variation of  $\phi_{non-SSW}$  appeared to be critically dependent on the energy balance of the leaf as controlled by g<sub>s H2O</sub>. In that, it seems possible that the CO<sub>2</sub>-dependent relationship between (w<sub>i</sub> - w<sub>a</sub>)/w<sub>a</sub> and  $\phi_{\text{non-SSW}}$  is somehow connected with the position (depth inside the leaf) of evaporative sites, and related effects on L, particularly at high humidity.

# 4.4 | Absence of a daytime RH effect on <sup>18</sup>O enrichment of leaf water—Unreal, uncommon or just unnoted and underexplored?

Commonly,  $\Delta^{18}O_{LW}$  exhibits a negative trend with RH (e.g., Cernusak et al., 2016, 2022; Helliker & Ehleringer, 2002; Hirl et al., 2019; Lehmann et al., 2017; Liu et al., 2017), a relation that we did not find here. But, we did find evidence of some effect of daytime evaporative conditions in bulk leaf water composition, based on the observations that the deuterium deviation with reference to the global meteoric water line (Voelker et al., 2014; Wei & Lee, 2019) was higher at low RH than at high RH, for all [CO<sub>2</sub>] levels (Figure 1, Supporting Information: Table S2).

The commonly expected relation between RH and  $\Delta^{18}O_{LW}$  is generally interpreted in terms of predictions from the Craig–Gordon model (e.g., Roden & Ehleringer, 1999), which dictates a strong negative effect of increasing RH on  $\Delta^{18}O_e$  (Equation 1) and propagation of this enrichment in leaf water (Barbour, 2007; Cernusak et al., 2016, 2022; Craig & Gordon, 1965; Dongmann et al., 1974; Farquhar et al., 1989, 2007; Flanagan et al., 1991). However, a recent compilation of published and previously unpublished leaf water isotope data (data set S1 in Cernusak et al., 2022) demonstrates an (RH-insensitive) global average  $\phi_{LW}$ 

of 0.16, which indicates that the RH sensitivity of  $\Delta^{18}O_{LW}$  should be about 16% smaller than that of  $\Delta^{18}O_e$ . However,  $\phi_{LW}$  can be much greater (Cernusak et al., 2016), which would further reduce the RH sensitivity of  $\Delta^{18} O_{LW}$  in these cases. Specifically, the grassland (Hirl et al., 2019) and grass species (Stipa capillata, Zhao et al., 2014) included in the Cernusak et al. (2022) data set had an average  $\varphi_{LW}$  of 0.36 and 0.45, respectively, suggesting per se a 36% and 45% reduced RH sensitivity of  $\Delta^{18}O_{LW}$  relative to  $\Delta^{18}O_{e}$ . Moreover,  $\phi_{LW}$ exhibited a common negative RH response of -0.005%<sup>-1</sup> in the studies of Hirl et al. (2019) and Zhao et al. (2014) (data collected between 10 AM and 4 PM), respectively (Supporting Information: Figure \$4), a fact not highlighted or discussed before. This negative RH response of  $\phi_{LW}$  implied an additional 13% reduction of the RH effect on  $\Delta^{18}O_{LW}$  in the range from 50% to 75% RH. In the present work, we observed a mean  $\phi_{LW}$  of 0.37 and an RH-sensitivity of  $\phi_{LW}$ (-0.01%<sup>-1</sup>) which was twice that of Hirl et al. (2019) and Zhao et al. (2014). This greater negative RH response of  $\phi_{LW}$  effectively cancelled the RH effect on  $\Delta^{18}O_{LW}$  in our investigations and was mainly related to the opposite effects of RH on  $\Delta^{18}O_{non-SSW}$  relative to  $\Delta^{18}O_{SSW}$ . Notably, other datasets with a nonsignificant RH response of  $\Delta^{18}O_{LW}$  are also included in the data set of Cernusak et al. (2022) and comprise the S. capillata data of Zhao et al. (2014; samples collected between 10 AM and 4 PM and reflecting an RH range from 26% to 56%). Notably, the RH sensitivity of  $\Delta^{18}O_{LW}$ which we calculate from the data of Lehmann et al. (2017) is also quite low, when compared to the average response of the global data set of Cernusak et al. (2022): -0.09%/% versus -0.30%/%. These findings and considerations all support the view that the magnitude and range of the  $\phi_{LW}$  and  $\Delta^{18}O_{LW}$  data and their response to RH, as observed in the present work, fall inside the range of observations made previously by others in diverse environments (Cernusak et al., 2022).

# 5 | CONCLUSION AND OUTLOOK

This work demonstrated that  $\Delta^{18} O_{SSW}$  was well predicted by  $\Delta^{18} O_{\rm e}$ with offsets that correlated with gas exchange parameters (g<sub>s</sub> or total conductance to CO<sub>2</sub>) influenced by [CO<sub>2</sub>] in the growth environment. Offsets between  $\Delta^{18}O_{SSW}$  and  $\Delta^{18}O_{e}$  may have resulted from spatial gradients of evaporative <sup>18</sup>O enrichment in the mesophyll which diverged from spatial patterns of photosynthetic activity. Remarkably,  $\Delta^{18}O_{LW}$  was a poor predictor of  $\Delta^{18}O_{SSW}$ , as RH had an opposite effect on  $\Delta^{18}O_{non\text{-SSW}}$  relative to  $\Delta^{18}O_{SSW}$ . The effect of  $\Delta^{18}O_{non-SSW}$  on  $\Delta^{18}O_{LW}$  was strong, as the fraction of nonphotosynthetic tissue water in bulk leaf water was high, with epidermis water a dominant component. Leaf-to-air temperature gradients were mainly dependent on  $[CO_2]$  and had a strong effect on  $\phi_{non-SSW}$ , a phenomenon that correlated with the transpiration-to-water vapour influx ratio, particularly at high RH. Based on the present analysis, we believe that future work should target the following questions: (1) Which constitutive biophysical mechanisms determine the variation of  $\varphi_{SSW}$  and its relationship with  $g_s$ ,  $g_m$  and  $g_{total}$ ? (2) How do the

of use; OA articles are governed by the applicable Creative Commons

opposite effects of CO<sub>2</sub> and RH on the *E* vs *L* relationship affect the interpretation of  $\Delta^{18} O_{LW}$  signals, especially in the case of long-term timeseries (climate change); (3) Is RH sensitivity of  $\Delta^{18} O_{LW}$  influenced by leaf hydraulic design or energy balance? And how do these factors influence  $\Delta^{18} O_{non\text{-SSW}}$  in particular? And more generally; (4) which mechanisms underlie the natural variation of the RH sensitivity of  $\Delta^{18} O_{LW}$ , beyond effects of nonsteady-state, vapour isotope composition or boundary-layer and stomatal conductance?

### **ACKNOWLEDGEMENTS**

2646

We thank Anja Schmidt, Monika Michler, Angela Ernst-Schwärzli, Laura Dorn, Wolfgang Feneis, Richard Wenzel and Hans Vogl for skillful assistance in sampling and sample processing (A. S., M. M., A. E. S., H. V.), carbohydrate analyses (A. S., L. D.), maintenance of the mesocosm facility and gas exchange equipment (W. F., R. W.), and manufacturing thermocouples for leaf temperature measurements (R. W.). We acknowledge preliminary discussions with Haitao Liu (Henan Agricultural University, China) and Xiaoying Gong (Fujian Normal University, China), as well as comments of Rolf Siegwolf (Eidg. Forschungsanstalt für Wald, Schnee und Landschaft, WSL, Switzerland). Comments of Guillaume Tcherkez and two anonymous referees helped us greatly to improve the paper. This research was supported by the Deutsche Forschungsgemeinschaft (DFG SCHN 557/9-1). J. Z. was supported by the China Scholarship Council (CSC). Open Access funding enabled and organized by Projekt DEAL.

# CONFLICT OF INTEREST STATEMENT

The authors declare no conflict of interest

# DATA AVAILABILITY STATEMENT

The data sets that support the findings of this study are available from the corresponding author on reasonable request.

# ORCID

Juan C. Baca Cabrera 🕩 http://orcid.org/0000-0001-8159-3837

# REFERENCES

- Ainsworth, E.A. & Rogers, A. (2007) The response of photosynthesis and stomatal conductance to rising [CO<sub>2</sub>]: mechanisms and environmental interactions. *Plant, Cell & Environment*, 30, 258–270.
- Baca Cabrera, J.C., Hirl, R.T., Schäufele, R., Macdonald, A. & Schnyder, H. (2021) Stomatal conductance limited the CO<sub>2</sub> response of grassland in the last century. *BMC Biology*, 19, 50.
- Baca Cabrera, J.C., Hirl, R.T., Zhu, J., Schäufele, R. & Schnyder, H. (2020) Atmospheric CO<sub>2</sub> and VPD alter the diel oscillation of leaf elongation in perennial ryegrass: compensation of hydraulic limitation by stored-growth. New Phytologist, 227, 1776–1789.
- Barbour, M.M. (2007) Stable oxygen isotope composition of plant tissue: a review. Functional Plant Biology, 34, 83–94.
- Barbour, M.M. & Farquhar, G.D. (2004) Do pathways of water movement and leaf anatomical dimensions allow development of gradients in  ${\rm H_2}^{18}{\rm O}$  between veins and the sites of evaporation within leaves? *Plant, Cell & Environment*, 27, 107–121.
- Barbour, M.M., Farquhar, G.D. & Buckley, T.N. (2017) Leaf water stable isotopes and water transport outside the xylem. *Plant, Cell & Environment*, 40, 914–920.

- Barbour, M.M., Loucos, K.E., Lockhart, E.L., Shrestha, A., McCallum, D., Simonin, K.A. et al. (2021) Can hydraulic design explain patterns of leaf water isotopic enrichment in C<sub>3</sub> plants? *Plant*, *Cell & Environment*, 44, 432–444.
- Bernacchi, C.J., Singsaas, E.L., Pimentel, C., Portis, A.R. Jr. & Long, S.P. (2001) Improved temperature response functions for models of rubisco-limited photosynthesis. *Plant, Cell & Environment*, 24, 253–259.
- Braun, D.M., Wang, L. & Ruan, Y.-L. (2014) Understanding and manipulating sucrose phloem loading, unloading, metabolism, and signalling to enhance crop yield and food security. *Journal of Experimental Botany*, 65, 1713–1735.
- Cernusak, L.A., Barbeta, A., Bush, R.T., Eichstaedt (Bögelein), R., Ferrio, J.P., Flanagan, L.B. et al. (2022) Do <sup>2</sup>H and <sup>18</sup>O in leaf water reflect environmental drivers differently? *New Phytologist*, 235, 41–51.
- Cernusak, L.A., Barbour, M.M., Arndt, S.K., Cheesman, A.W., English, N.B., Feild, T.S. et al. (2016) Stable isotopes in leaf water of terrestrial plants. *Plant, Cell & Environment*, 39, 1087–1102.
- Cernusak, L.A., Farquhar, G.D. & Pate, J.S. (2005) Environmental and physiological controls over oxygen and carbon isotope composition of Tasmanian blue gum, *Eucalyptus globulus*. *Tree Physiology*, 25, 129–146.
- Cernusak, L.A., Wong, S.C. & Farquhar, G.D. (2003) Oxygen isotope composition of phloem sap in relation to leaf water in *Ricinus* communis. Functional Plant Biology, 30, 1059–1070.
- Chapman, D.F., Bryant, J.R., Olayemi, M.E., Edwards, G.R., Thorrold, B.S., McMillan, W.H. et al. (2017) An economically based evaluation index for perennial and short-term ryegrasses in New Zealand dairy farm systems. *Grass and Forage Science*, 72, 1–21.
- Charles-Edwards, D.A., Charles-Edwards, J. & Sant, F.I. (1974) Leaf photosynthetic activity in six temperate grass varieties grown in contrasting light and temperature environments. *Journal of Experimental Botany*, 25, 715–724.
- Cowan, I.R. & Farquhar, G.D. (1977) Stomatal function in relation to leaf metabolism and environment. Symposia of the Society for Experimental Biology, 31, 471–505.
- Craig, H. & Gordon, L.I. (1965) Deuterium and oxygen-18 variations in the ocean and marine atmosphere. In: Tongiorgi, E. (Ed.) Proceedings of conference on stable isotopes in oceanographic studies and palaeotemperatures. Pisa, Italy: Lischi and Figli, pp. 9-130.
- da Silveira Lobo O'Reilly Sternberg, L. & DeNiro, M.J.D. (1983) Biogeochemical implications of the isotopic equilibrium fractionation factor between the oxygen atoms of acetone and water. Geochimica et Cosmochimica Acta, 47, 2271–2274.
- Dengler, N. (1994) Quantitative leaf anatomy of C3 and C4 grasses (poaceae): bundle sheath and mesophyll surface area relationships. Annals of Botany, 73, 241–255.
- DeNiro, M.J. & Epstein, S. (1981) Isotopic composition of cellulose from aquatic organisms. *Geochimica et Cosmochimica Acta*, 45, 1885–1894.
- Dongmann, G., Nürnberg, H.W., Förstel, H. & Wagener, K. (1974) On the enrichment of  ${\rm H_2}^{18}{\rm O}$  in the leaves of transpiring plants. *Radiation and Environmental Biophysics*, 11, 41–52.
- Epstein, S., Thompson, P. & Yapp, C.J. (1977) Oxygen and hydrogen isotopic ratios in plant cellulose. *Science*, 198, 1209–1215.
- Evans, J., Sharkey, T., Berry, J. & Farquhar, G. (1986) Carbon isotope discrimination measured concurrently with gas exchange to investigate CO<sub>2</sub> diffusion in leaves of higher plants. *Functional Plant Biology*, 13, 281–292.
- Farquhar, G.D. & Cernusak, L.A. (2012) Ternary effects on the gas exchange of isotopologues of carbon dioxide. *Plant*, *Cell* & *Environment*, 35, 1221–1231.
- Farquhar, G.D., Cernusak, L.A. & Barnes, B. (2007) Heavy water fractionation during transpiration. *Plant Physiology*, 143, 11–18.



- Farquhar, G.D. & Gan, K.S. (2003) On the progressive enrichment of the oxygen isotopic composition of water along a leaf. *Plant*, *Cell & Environment*, 26, 801–819.
- Farquhar, G.D., Hubick, K., Condon, A. & Richards, R. (1989) Carbon isotope fractionation and plant water-use efficiency. In: Rundel, P.W., Ehleringer, J.R. & Nagy, K.A. (Eds.) Stable isotopes in ecological research. New York: Springer, pp. 21–40.
- Farquhar, G.D. & Lloyd, J. (1993) Carbon and oxygen isotope effects in the exchange of carbon dioxide between terrestrial plants and the atmosphere. In: Ehleringer, J.R., Hall, A.E. & Farquhar, G.D. (Eds.) Stable isotopes and plant carbon-water relations. San Diego: Academic Press. pp. 47–70.
- Farquhar, G.D., O'Leary, M.H. & Berry, J.A. (1982) On the relationship between carbon isotope discrimination and the intercellular carbon dioxide concentration in leaves. Australian Journal of Plant Physiology, 9, 121–137.
- Ferrio, J.P., Pou, A., Florez-Sarasa, I., Gessler, A., Kodama, N., Flexas, J. et al. (2012) The Péclet effect on leaf water enrichment correlates with leaf hydraulic conductance and mesophyll conductance for CO<sub>2</sub>. Plant, Cell & Environment, 35, 611–625.
- Flanagan, L.B., Comstock, J.P. & Ehleringer, J.R. (1991) Comparison of modeled and observed environmental influences on the stable oxygen and hydrogen isotope composition of leaf water in *Phaseolus vulgaris* L. *Plant Physiology*, 96, 588–596.
- Flexas, J., Scoffoni, C., Gago, J. & Sack, L. (2013) Leaf mesophyll conductance and leaf hydraulic conductance: an introduction to their measurement and coordination. *Journal of Experimental Botany*, 64, 3965–3981.
- Franks, P.J. & Beerling, D.J. 2009. Maximum leaf conductance driven by CO<sub>2</sub> effects on stomatal size and density over geologic time. Proceedings of the National Academy of Sciences, 106, 10343–10347.
- Gan, K.S., Wong, S.C., Yong, J.W.H. & Farquhar, G.D. (2002) <sup>18</sup>O spatial patterns of vein xylem water, leaf water, and dry matter in cotton leaves. *Plant Physiology*, 130, 1008–1021.
- Gan, K.S., Wong, S.C., Yong, J.W.H. & Farquhar, G.D. (2003) Evaluation of models of leaf water <sup>18</sup>O enrichment using measurements of spatial patterns of vein xylem water, leaf water and dry matter in maize leaves. *Plant, Cell & Environment*, 26, 1479–1495.
- Garnier, E. & Laurent, G. (1994) Leaf anatomy, specific mass and water content in congeneric annual and perennial grass species. New Phytologist, 128, 725–736.
- Gebbing, T. & Schnyder, H. (2001)  $^{13}$ C labeling kinetics of sucrose in glumes indicates significant refixation of respiratory  $CO_2$  in the wheat ear. Functional Plant Biology, 28, 1047–1053.
- Gong, X.Y., Schäufele, R., Feneis, W. & Schnyder, H. (2015) <sup>13</sup>CO<sub>2</sub>/<sup>12</sup>CO<sub>2</sub> exchange fluxes in a clamp-on leaf cuvette: disentangling artefacts and flux components. *Plant, Cell & Environment*, 38, 2417–2432.
- Grace, J. & Wilson, J. (1976) The boundary layer over a *Populus* leaf. *Journal of Experimental Botany*, 27, 231–241.
- Helliker, B.R. & Ehleringer, J.R. (2000) Establishing a grassland signature in veins:  $^{18}$ O in the leaf water of  $C_3$  and  $C_4$  grasses. *Proceedings of the National Academy of Science*, 97, 7894–7898.
- Helliker, B.R. & Ehleringer, J.R. (2002) Differential  $^{18}O$  enrichment of leaf cellulose in  $C_3$  versus  $C_4$  grasses. Functional Plant Biology, 29, 435–442.
- Hetherington, A.M. & Woodward, F.I. (2003) The role of stomata in sensing and driving environmental change. *Nature*, 424, 901–908.
- Hirl, R.T., Ogée, J., Ostler, U., Schäufele, R., Baca Cabrera, J.C., Zhu, J. et al. (2021) Temperature-sensitive biochemical  $^{18}\text{O-fractionation}$  and humidity-dependent attenuation factor are needed to predict  $\delta^{18}\text{O}$  of cellulose from leaf water in a grassland ecosystem. New Phytologist, 229, 3156–3171.
- Hirl, R.T., Schnyder, H., Ostler, U., Schäufele, R., Schleip, I., Vetter, S.H. et al. (2019) The <sup>18</sup>O ecohydrology of a grassland ecosystem—

- predictions and observations. *Hydrology and Earth System Sciences*, 23, 2581–2600.
- Holloway-Phillips, M., Baan, J., Nelson, D.B., Lehmann, M.M., Tcherkez, G., & Kahmen, A. (2022) Species variation in the hydrogen isotope composition of leaf cellulose is mostly driven by isotopic variation in leaf sucrose. *Plant, Cell & Environment*, 45, 2636–2651. https://doi. org/10.1111/pce.14362
- Holloway-Phillips, M., Cernusak, L.A., Barbour, M., Song, X., Cheesman, A., Munksgaard, N. et al. (2016) Leaf vein fraction influences the Péclet effect and <sup>18</sup>O enrichment in leaf water. *Plant, Cell & Environment*, 39, 2414–2427.
- Koroleva, O.A., Farrar, J.F., Deri Tomos, A. & Pollock, C.J. (1998) Carbohydrates in individual cells of epidermis, mesophyll, and bundle sheath in barley leaves with changed export or photosynthetic rate. *Plant Physiology*, 118, 1525–1532.
- Lalonde, S., Tegeder, M., Throne-Holst, M., Frommer, W.B. & Patrick, J.W. (2003) Phloem loading and unloading of sugars and amino acids. *Plant, Cell & Environment*, 26, 37–56.
- Lanigan, G.J., Betson, N., Griffiths, H. & Seibt, U. (2008) Carbon isotope fractionation during photorespiration and carboxylation in Senecio. Plant Physiology, 148, 2013–2020.
- Larcher, L., Hara-Nishimura, I. & Sternberg, L. (2015) Effects of stomatal density and leaf water content on the <sup>18</sup>O enrichment of leaf water. *New Phytologist*, 206, 141–151.
- Lattanzi, F.A., Ostler, U., Wild, M., Morvan-Bertrand, A., Decau, M.-L., Lehmeier, C.A. et al. (2012) Fluxes in central carbohydrate metabolism of source leaves in a fructan-storing C<sub>3</sub> grass: rapid turnover and futile cycling of sucrose in continuous light under contrasted nitrogen nutrition status. *Journal of Experimental Botany*, 63, 2363–2375.
- Leaney, F.W., Osmond, C.B., Allison, G.B. & Ziegler, H. (1985) Hydrogenisotope composition of leaf water in  $C_3$  and  $C_4$  plants: its relationship to the hydrogen-isotope composition of dry matter. *Planta*, 164, 215–220.
- Lehmann, M.M., Gamarra, B., Kahmen, A., Siegwolf, R. & Saurer, M. (2017) Oxygen isotope fractionations across individual leaf carbohydrates in grass and tree species. *Plant, Cell & Environment*, 40, 1658–1670.
- Liu, H.T., Gong, X.Y., Schäufele, R., Yang, F., Hirl, R.T., Schmidt, A. et al. (2016) Nitrogen fertilization and  $\delta^{18}$ O of CO<sub>2</sub> have no effect on  $^{18}$ O-enrichment of leaf water and cellulose in *Cleistogenes squarrosa* (C<sub>4</sub>) —is VPD the sole control? *Plant, Cell & Environment*, 39, 2701–2712.
- Liu, H.T., Schäufele, R., Gong, X.Y. & Schnyder, H. (2017) The  $\delta^{18}O$  and  $\delta^{2}H$  of water in the leaf growth-and-differentiation zone of grasses is close to source water in both humid and dry atmospheres. *New Phytologist*, 214, 1423–1431.
- Loucos, K.E., Simonin, K.A., Song, X. & Barbour, M.M. (2015) Observed relationships between leaf H<sub>2</sub><sup>18</sup>O Peclet effective length and leaf hydraulic conductance reflect assumptions in Craig-Gordon model calculations. *Tree Physiology*, 35, 16-26.
- Ma, W.T., Tcherkez, G., Wang, X.M., Schäufele, R., Schnyder, H., Yang, Y. et al. (2021) Accounting for mesophyll conductance substantially improves <sup>13</sup>C-based estimates of intrinsic water-use efficiency. New Phytologist, 229, 1326–1338.
- Majoube, M. (1971) Fractionnement en oxygène 18 et en deutérium entre l'eau et sa vapeur. *Journal de Chimie Physique*, 68, 1423–1436.
- McNevin, D.B., Badger, M.R., Kane, H.J. & Farquhar, G.D. (2006) Measurement of (carbon) kinetic isotope effect by Rayleigh fractionation using membrane inlet mass spectrometry for CO<sub>2</sub>consuming reactions. *Functional Plant Biology*, 33, 1115–1128.
- Meinzer, F.C. & Saliendra, N.Z. (1997) Spatial patterns of carbon isotope discrimination and allocation of photosynthetic activity in sugarcane leaves. Functional Plant Biology, 24, 769–775.
- O'Leary, M.H. (1984) Measurement of the isotope fractionation associated with diffusion of carbon dioxide in aqueous solution. *The Journal of Physical Chemistry*, 88, 823–825.

Plant, Cell & Environment, 35, 1040-1049.

- Ocheltree, T.W., Nippert, J.B. & Prasad, P.V.V. (2012) Changes in stomatal conductance along grass blades reflect changes in leaf structure.
- Ogée, J., Cuntz, M., Peylin, P. & Bariac, T. (2007) Non-steady-state, nonuniform transpiration rate and leaf anatomy effects on the progressive stable isotope enrichment of leaf water along monocot leaves. *Plant, Cell & Environment*, 30, 367–387.
- Pinheiro, J., Bates, D., DebRoy, S., Sarkar, D. & Core Team, R. 2019. nlme: linear and nonlinear mixed effects model. R package version 3.1–141
- Pollock, C.J. & Cairns, A.J. (1991) Fructan metabolism in grasses and cereals. Annual Review of Plant Physiology and Plant Molecular Biology, 42, 77–101.
- Poorter, H., Knopf, O., Wright, I.J., Temme, A.A., Hogewoning, S.W., Graf, A. et al. (2022) A meta-analysis of responses of C<sub>3</sub> plants to atmospheric CO<sub>2</sub>: dose-response curves for 85 traits ranging from the molecular to the whole-plant level. *New Phytologist*, 233, 1560–1596.
- R Core Team. 2022. R: a language and environment for statistical computing.

  Vienna, Austria: R Foundation for Statistical Computing.
- Rockwell, F.E., Holbrook, N.M. & Stroock, A.D. (2014) The competition between liquid and vapor transport in transpiring leaves. *Plant Physiology*, 164, 1741–1758.
- Roden, J.S. & Ehleringer, J.R. (1999) Observations of hydrogen and oxygen isotopes in leaf water confirm the Craig-Gordon model under wideranging environmental conditions. *Plant Physiology*, 120, 1165–1174.
- Schneider, C.A., Rasband, W.S. & Eliceiri, K.W. (2012) NIH image to ImageJ: 25 years of image analysis. *Nature Methods*, 9, 671–675.
- Siegwolf, R.T., Brooks, J.R., Roden, J., & Saurer, M. (2022) Stable isotopes in tree rings: inferring physiological, climatic and environmental responses. Springer Nature.
- Smith, J.A.C. & Milburn, J.A. (1980) Osmoregulation and the control of phloem-sap composition in *Ricinus communis L. Planta*, 148, 28–34.
- Song, X., Barbour, M.M., Farquhar, G.D., Vann, D.R. & Helliker, B.R. (2013) Transpiration rate relates to within- and across-species variations in effective path length in a leaf water model of oxygen isotope enrichment. Plant, Cell & Environment, 36, 1338–1351.
- Song, X., Loucos, K.E., Simonin, K.A., Farquhar, G.D. & Barbour, M.M. (2015) Measurements of transpiration isotopologues and leaf water to assess enrichment models in cotton. *New Phytologist*, 206, 637–646.
- Sternberg, L. & Ellsworth, P.F.V. (2011) Divergent biochemical fractionation, not convergent temperature, explains cellulose oxygen isotope enrichment across latitudes. *PLoS One*, 6, e28040.
- Sternberg, L.S.L. & Manganiello, L.M. (2014) Stomatal pore size and density in mangrove leaves and artificial leaves: effects on leaf water isotopic enrichment during transpiration. Functional Plant Biology, 41, 648–658.
- Ubierna, N., Holloway-Phillips, M.-M. & Farquhar, G.D. (2018) Using stable carbon isotopes to study  $C_3$  and  $C_4$  photosynthesis: models and calculations. In: Covshoff, S. (Ed.) *Photosynthesis: methods and protocols.* New York, NY: Springer New York, pp. 155–196.

- Voelker, S.L., Brooks, J.R., Meinzer, F.C., Roden, J., Pazdur, A., Pawelczyk, S. et al. (2014) Reconstructing relative humidity from plant  $\delta^{18}$ O and  $\delta D$  as deuterium deviations from the global meteoric water line. *Ecological Applications*, 24, 960–975.
- Wagner, W., Keller, F. & Wiemken, A. (1983) Fructan metabolism in cereals: induction in leaves and compartmentation in protoplasts and vacuoles. *Zeitschrift für Pflanzenphysiologie*, 112, 359–372.
- Wei, Z. & Lee, X. (2019) The utility of near-surface water vapor deuterium excess as an indicator of atmospheric moisture source. *Journal of Hydrology*, 577, 123923.
- Wickham, H. (2016) ggplot2: Elegant Graphics for Data Analysis. New York: Springer Verlag.
- Winter, H., Robinson, D. & Heldt, H. (1993) Subcellular volumes and metabolite concentrations in barley leaves. *Planta*, 191, 180-190.
- Xiong, D., Yu, T., Liu, X., Li, Y., Peng, S. & Huang, J. (2015) Heterogeneity of photosynthesis within leaves is associated with alteration of leaf structural features and leaf N content per leaf area in rice. Functional Plant Biology, 42, 687–696.
- Yakir, D., Berry, J.A., Giles, L. & Osmond, C.B. (1994) Isotopic heterogeneity of water in transpiring leaves: identification of the component that controls the  $\delta^{18}O$  of atmospheric  $O_2$  and  $CO_2$ . Plant, Cell & Environment, 17, 73–80.
- Yakir, D. & DeNiro, M.J. (1990) Oxygen and hydrogen isotope fractionation during cellulose metabolism in *Lemna gibba* L. *Plant Physiology*, 93, 325–332.
- Yakir, D., DeNiro, M.J. & Gat, J.R. (1990) Natural deuterium and oxygen-18 enrichment in leaf water of cotton plants grown under wet and dry conditions: evidence for water compartmentation and its dynamics. Plant, Cell & Environment, 13, 49–56.
- Zhao, L., Wang, L., Liu, X., Xiao, H., Ruan, Y. & Zhou, M. (2014) The patterns and implications of diurnal variations in the d-excess of plant water, shallow soil water and air moisture. *Hydrology and Earth System Sciences*, 18, 4129–4151.
- Zwieniecki, M.A., Brodribb, T.J. & Holbrook, N.M. (2007) Hydraulic design of leaves: insights from rehydration kinetics. *Plant, Cell & Environment*, 30, 910–921.

### SUPPORTING INFORMATION

Additional supporting information can be found online in the Supporting Information section at the end of this article.

**How to cite this article:** Baca Cabrera, J. C., Hirl, R. T., Zhu, J., Schäufele, R., Ogée, J. & Schnyder, H. (2023)  $^{18}$ O enrichment of sucrose and photosynthetic and nonphotosynthetic leaf water in a  $C_3$  grass—atmospheric drivers and physiological relations. *Plant, Cell & Environment*, 46, 2628–2648.

https://doi.org/10.1111/pce.14655